rat CD1d are designated as P80rCD80rCD1d, those transduced with mouse CD1d as P80rCD80mCD1d.

Mouse CD1d was cloned from A20mCD1d cell line (38) by RT-PCR using the following primers: mCD1d-*Eco*RI-Fow (5′-GGG GAG AAT TCC GGC GCT ATG CGG TAC CTA CC-3′); and mCD1d-*Eco*RI-Rev (5′-GGT GGA ATT CAG AGT CAC CGG ATG TCT TGA TAA G-3′). The sequence of the insert showed a complete overlap with the mouse CD1d sequence available in the gene bank under X13170 (39). Rat CD1d cDNA was obtained by RT-PCR using RNA isolated from F344/Crl rat bone marrow as a template and CD1d-specific primers: N366 (5′-TCG GAG CCC AGG GCT GTG TAG A-3′); and rCD1dRev (5′-TTC TGA GCA GAC AAG GAC TGA-3′). PCR product was cloned into TOPO cloning vector and sequenced. The sequence was identical with rat CD1d (GenBank accession number AB029486) published by Katabami et al. (23). Mouse and rat CD1d DNA were cloned into *Eco*RI site of pczCGZ5IZ and pczCGZ5 IEGZ vectors, respectively, and were further used for retroviral infection of P80rCD80 cells.

The expression of mouse CD1d was tested with the CD1d-specific mAb 1B1 (BD Pharmingen), whereas expression of rat CD1d was assessed from the green fluorescence of the *EGFP* reporter gene. Surface expression of rat CD1d was also confirmed with a novel rat CD1d-specific mAb (E. Pyz and T. Herrmann, unpublished observations). The Ag-presenting cell lines were enriched for CD1d expression by cell sorting or selection with antibiotics.

Stimulation with α-GalCer in vitro

α-GalCer was generated as described (40). The reactivity of mouse and rat IHLs to α-GalCer was tested by culture of IHL (1×10^5 cells/well of a 96-well round-bottom plate) in the presence of α-GalCer (100 ng/ml), vehicle (DMSO), or complete medium for 24 h at 37°C. The level of IL-4 and IFN-γ released into culture supernatants was determined using ELISA kits (BD Pharmingen).

To analyze the α-GalCer reactivity of TCR-transduced cell lines, mouse and rat thymocytes (1×10^6 cells/well), or CD1d-transduced cells (P80mCD1drCD80, P80rCD1drCD80, 5×10^4 cell/well) used as APC were loaded with either α-GalCer (1–100 ng/ml) or vehicle (DMSO) for 1–2 h before the addition of responder cells. As a positive control, TCR-positive cell lines were stimulated with plate-bound anti-mouse CD3 mAb 145C11. After 24 h of culture, supernatants were taken, and the secreted mouse IL-2 was quantified using a commercial ELISA Kit (BD Pharmingen).

Immunofluorescence and flow cytometry

For the staining, 2×10^5 cells were diluted in 100 μl of FACS buffer (PBS (pH7.4), 0.1% BSA, 0.02% NaN_3) and were treated for 10 min at 4°C with normal mouse Ig (Sigma-Aldrich) or mouse FcγR-specific 2.4G2 Ab to block unspecific binding or binding to Fc receptors. Subsequently, cells were stained for 30 min with labeled mAbs, washed, and stained with another mAb or analyzed with a FACScan or FACSCalibur flow cytometer (BD Biosciences).

All mouse and rat mAbs were obtained from BD Pharmingen and are given with their clone names: mouse Vβ8.1, 8.2, 8.3 (F23.1); mouse CD3 ε-chain (145-C11); mouse CD1d (1B1); mouse CD4 (GK1.5); mouse CD8α (53-6.7); NK1.1 (PK136); BV8S4A1 and BV8S4A2, Vβ8.2 of LEW rats and Vβ8.4 of F344/Crl rat (R78); rat TCR β-chain (R73); rat CD4 (W3/25); rat CD4 (OX35); rat CD8β (3.4.1.); rat NKR-P1A (10-78). Abs were usually FITC or PE labeled. Biotinylated mAbs, when used, were visualized with streptavidin-CyChrome. Unconjugated Abs, used in indirect immunofluorescent staining, were detected by using fluorochrome-conjugated Abs: PE- or Cy5.5-conjugated $(Fab')_2$ fragment of donkey anti-mouse IgG or goat anti-hamster IgG FITC obtained from Dianova or Serotec).

Staining with α-GalCer-loaded mouse CD1d-PE tetramer

α-GalCer-loaded or control mouse CD1d-PE tetramers were generated as described in Ref. 18. Tetramer staining of mouse/rat IHL- or TCR-transduced cell lines was performed as normal FACS staining, but with incubation for 1 h at room temperature. Tetramer concentrations were 350 (high tetramer) or 35 ng/50 μl cell suspension (low tetramer).

Results

Phenotype and α-GalCer response of rat IHL

In mouse and human, the highest proportion iNKT cells can be found among intrahepatic lymphocytes. In an attempt to identify the corresponding population in rat, IHL of F344/Crl rats and C57BL/6 mice were compared for cell surface phenotype (Fig. 1*A*), binding of α-Gal-loaded mouse CD1d tetramers (Fig. 1*B*), and α-GalCer-induced cytokine production (Fig. 1*C*). In agreement with published data, about one-third of mouse IHL coexpressed NK1.1 (mouse homolog to rat NKR-P1A) and TCR. More than 20% of IHL coexpressed NK1.1 and CD4, but very few coexpressed NK1.1 and CD8αβ. As shown in Fig. 1*B*, ~27% of IHL show costaining of α-GalCer-loaded CD1d tetramer and anti-CD3, with the tetramer positive cells having a lower or intermediate level of expression of CD3. 25.5% of IHL were costained by tetramer and anti-NK1.1 (data not shown) and 20.4% by tetramer and anti-CD4, whereas only very few (0.38%) stained with CD1d tetramer and CD8-specific mAb (data not shown).

The phenotypes of rat and mouse IHL differed considerably. First of all, <5% of rat IHL coexpressed NKR-P1A and CD3, and most of these cells were positive for CD8αβ but not for CD4, and they did not express intermediate CD3 levels. Secondly, in contrast to results found in mice, only a very small number of $CD3^+$ rat IHL were stained with α-GalCer-loaded mouse CD1d tetramer;

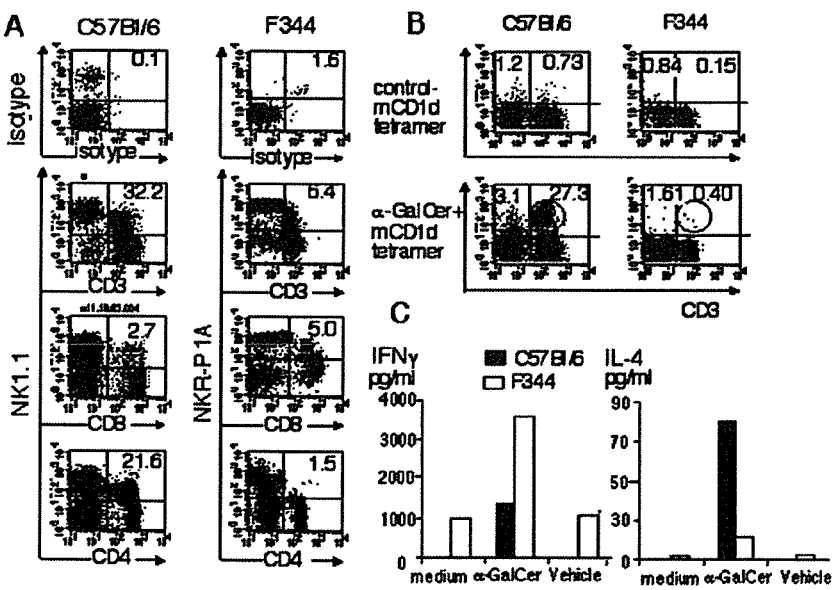

FIGURE 1. Phenotypic and functional analysis of typical iNKT cell features of C57BL/6 mouse and F344/Crl rat IHL. *A*, Two-color flow cytometry for coexpression of NK1.1 or NKR-P1A and indicated T cell markers. Percent of positive cells are indicated by numbers in the *upper right quadrant*. *B*, Two-color flow cytometry for binding of α-GalCer-loaded or unloaded mouse CD1d tetramers to $CD3^+$ positive (*upper right quadrant*) or $CD3^-$ (*upper left quadrant*) C57BL/6 mouse or F344/Crl rat IHL. Percentages of tetramer-positive cells are given in the respective quadrants. *C*, IFN-γ or IL-4 secretion during 24-h stimulation of 1×10^5 rat or mouse IHL with 100 ng/ml α-GalCer dissolved in DMSO, vehicle (DMSO alone), or medium alone. *Ordinate*, Cytokine concentration in picograms per milliliter.

0.4% of IHL were stained with α-GalCer-loaded tetramer and 0.15% with control tetramer. Even higher proportions of $CD3^-$ lymphocytes were stained by α-GalCer-loaded tetramers (1.61%) or control tetramers (0.84%), which made it likely that (much of) the tetramer staining of $CD3^+$ rat IHL was unspecific.

To test whether the lack of binding of mouse CD1d tetramer to rat IHL was due to the absence of α-GalCer-specific cells in F344/Crl rat liver, the α-GalCer reactivity of F344/Crl and C57BL/6 IHL (Fig. 1*C*) was compared. After 24 h of stimulation with α-GalCer (100 ng/ml), mouse and rat liver lymphocytes produced both IFN-γ and IL-4. The amount of rat IL-4 reached ~15% of that secreted by mouse cells. The IFN-γ production by rat IHL exceeded that of mouse IHL, but rat IHL showed also a high level of background IFN-γ production.

The α-GalCer-induced activation of cytokine production in conjunction with the detection of AV14AJ18 rearrangements in rat IHL strongly support the existence of an iNKT cell population in F344/Crl rats, although these cells could not be detected by mouse CD1d tetramer. This could be a consequence of 1) an extremely low frequency of rat iNKT cells and/or 2) a requirement for presentation of α-GalCer by syngeneic CD1d (species specificity), which finally would result in a lack of binding of mouse CD1d tetramers to rat iNKT TCR. To test the latter hypothesis, iNKT TCRs were cloned and expressed in TCR-negative BW58r/mCD28 cells and tested for mouse CD1d tetramer binding. In addition, these lines as well as lines expressing iNKT TCR variants were tested for reactivity to α-GalCer presented by mouse or rat CD1d.

Cloning and transduction of mouse and rat CD1d and iNKT TCR

Cloning, transduction, and quantification of surface expression of iNKT TCR was performed as described in *Materials and Methods*. Three AV14 α-chains were cloned into a retroviral vector carrying an *EGFP* as reporter gene. Two of them comprised V-encoded amino acid sequences identical with that of rat AV14S1 and rat AV14S8. The mouse AV14S1A2-chain was cloned from the α-GalCer-reactive mouse C57BL/6-derived iNKT cell hybridoma KT12. All AV14 α-chains were coexpressed with different mouse or rat BV8S2 β-chains, the properties of which will be discussed later in this section.

The sequences of the tested iNKT TCR α-chains are compared in the upper part of Fig. 2. Both rat AV14S1 and rat AV14S8 α-chain comprise type 1 AV14 sequences. The V domain of the rat AV14S1 α-chain is identical with sequences previously found by Matsuura et al. in F344/Crl rat liver (6). The rat AV14S8 α-chain sequence was directly cloned from F344/Crl IHL, as described in *Materials and Methods*. AV14S8 has not yet been described for F344/Crl rats, but an identical sequence has been found in the BN/SsNHsd rat genome, where it has been named AV14S8 (25). A peculiarity of the AV14S8-comprising α-chain used in this study may be the valine located at position 93 of the VJ junction which corresponds to the adult type of AV14AJ18 rearrangements (26). Otherwise, the mature Vα domains of the two rat TCRs differed by the following substitutions: K1R, Q15E, and K51T.

The middle part of Fig. 2 aligns the sequences of the TCR β-chains used in this study. The BV8S2-positive mouse β-chain was originally isolated from the iNKT T cell hybridoma KT12. The rat BV8S2 (BV8S2A1 or Tcrb-V8.2[1])-comprising β-chain used in this study was derived from the rat T cell hybridoma 35/1, which was generated with an encephalitogenic cell line of LEW/Crl origin as fusion partner. The 35/1 TCR is $RT1B^1$-restricted $gpMBP_{68-88}$ specific and reacts also with the superantigens of *Yersinia pseudotuberculosis* and *Mycoplasma arthritidis* and the staphylococcal enterotoxins B and C1 (33). As previously described in some detail (33), replacement of the CDR2 and/or the CDR4/HV4 of the BV8S4A2 with those of F344/Crl rats had distinct effects on (super)Ag reactivity. Changes in the CDR2 abolished reactivity for peptide Ag and staphylococcal enterotoxins B and C1, whereas mutation of the HV4/CDR4 affected only the response to staphylococcal enterotoxins (33). The β-chain containing the mutations within CDR2 and CDR4 is, with exception of a lacking L14K substitution, identical with the BV8S4A2 of F344/Crl rats. It lost specificity for the peptide Ag, staphylococcal enterotoxins and the superantigen of *M. arthritidis* (33).

The lower part of Fig. 2 presents the amino acid sequence of the α-1 and α-2 domains of rat and mouse CD1d. The α-helical parts

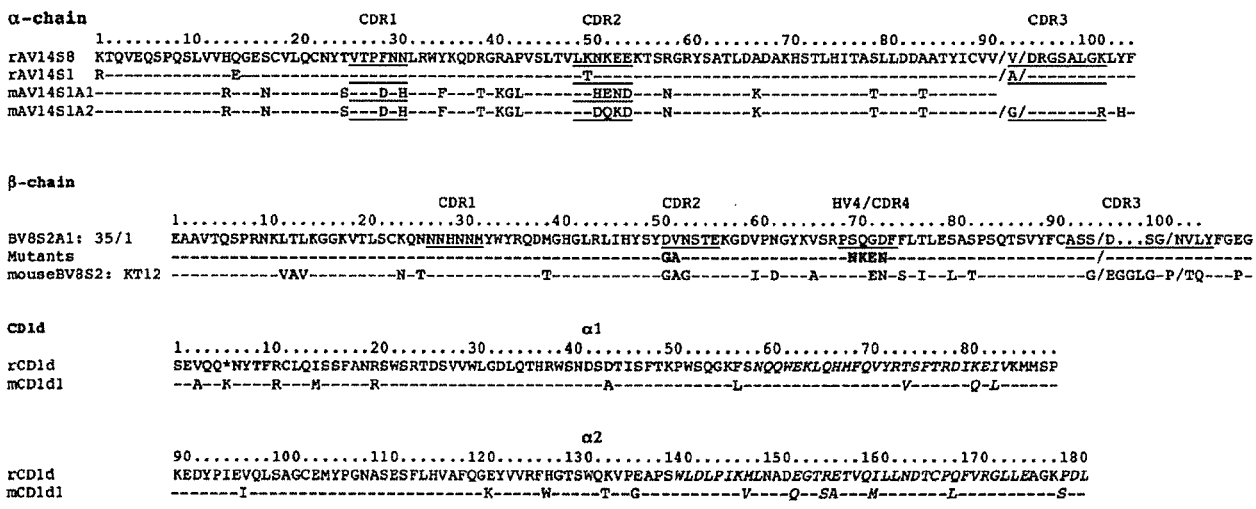

FIGURE 2. Alignment of amino acid sequences of the mature peptides TCR chain proteins (α-chain and β-chain) and CD1d molecules used or discussed in this study. Underlined parts of the TCR sequences indicate localization of CDRs. Parts of CD1d sequences in italics indicate α-helical regions. Amino acid sequences were deduced from the nucleotide sequences, the accession numbers of which can be found in GenBank: rAV14S8 α-chain, DQ340291; rAV14S1 α-chain, DQ340293; mAV14S1, AY158221; mAV14S1A2 (KT12 hybridoma), DQ340292; BV8S2A1 TCR35/1 β-chain, AY228549. Mutants entry indicates localization of the CDR2 and CDR4/HV4 substitutions introduced in the TCR35/1 β-chain, which are highlighted by bold letters. mBV8S2 TCR KT12, DQ340294; mCD1d (mouse CD1d), X13170.1; rCD1d (rat CD1d), AB029486.

of CD1d are marked. The α helices of the α1 domains differ in 3 aa. Visualization of the of the PDB files 1ZHN (10) and 1Z5L (12) of the mouse CD1d crystal structure by Swiss-PDB-viewer (http://swissmodel.expasy.org/SM_TOPPAGE.html) shows that T74 points upwards and K81 outwards, defining them as theoretical contact sites with the TCR. I83 points into the binding groove. The α-helical parts of the α-2 domain differ by 7 aa. With exception of the R157S, side chains of all substitutions show upwards and provide possible contacts for the TCR. In contrast to the differences in potential TCR contacts, those amino acids shown to provide H bonds with α-GalCer are conserved (12). Both *CD1d* genes were expressed in P815 cells (P80rCD80) overexpressing rat CD80 as described in *Materials and Methods*.

Species specificity of CD1d restriction in Ag recognition by rat iNKT TCR

First, we tested three responder cell lines for their α-GalCer reactivity and their capacity to bind mouse CD1d tetramers. The lines were BWr/mCD28 cells expressing: 1) as positive control, mouse iNKT TCR isolated from the KT12 hybridoma which consisted of a mouse AV14S1A2 α-chain and mouse BV8S2 β-chain; 2) rat AV14S1 α-chain with the CDR2+4 β-chain mutant; 3) the rat AV14S8 α-chain with the same β-chain mutant. The BV8S4-like CDR2+4 β-chain mutant was used, because there is circumstantial evidence that in F344/Crl rats, iNKT cells express the BV8S4-comprising β-chains (6). The two rat TCR lines expressed very similar levels of TCR, whereas expression of the mouse TCR was considerably lower (Fig. 3). Cell lines were tested three to five times for their α-GalCer-induced IL-2 secretion. IL-2 levels after CD3 ligation were quite similar, with the exception of sometimes considerably lower IL-2 production by the mouse iNKT TCR-transduced line (data not shown). Fig. 3 shows data from one representative assay of α-GalCer-induced IL-2 secretion. The APC-type thymocytes vs CD1d-transduced P80 cells and the origin of the transduced CD1d (rat vs mouse) considerably affected the outcome of the assay. Generally, with CD1d-transduced P80rCD80 cells as APC, Il-2 production was much higher than with thymocytes. This may reflect the differences in the level of CD1d and CD80 surface expression in primary vs CD1d-transduced cells (data not shown). In assays with mouse thymocytes as APC, some background IL-2 production was found, even if TCR-negative BW58 cells were used as responders, suggesting that IL-2 was secreted by α-GalCer-stimulated thymocytes (Figs. 3 and 5). With regard to a possible species specificity in CD1d-restricted α-GalCer recognition, all three lines responded to α-GalCer presented by rat CD1d-expressing cells, whereas α-GalCer mouse CD1d complexes stimulated only mouse iNKT TCR responder cells. In addition, the stimulation of the line expressing the rat AV14S1 α-chain was considerably stronger than of the rat AV14S8 α-chain-expressing line.

The differences in the response to α-GalCer presented by mouse CD1d correlated with the pattern of mouse CD1d tetramer staining as is shown in Fig. 3 Binding of mouse CD1d tetramers was normalized by dividing mean fluorescence intensity (MFI) of tetramer staining, through MFI of CD3 staining. After normalization, tetramer staining of the mouse iNKT TCR-expressing line was 24-fold, respectively, 8-fold stronger than that of the rat AV14S8 α-chain-expressing line or the rat AV14S1 α-chain-expressing line.

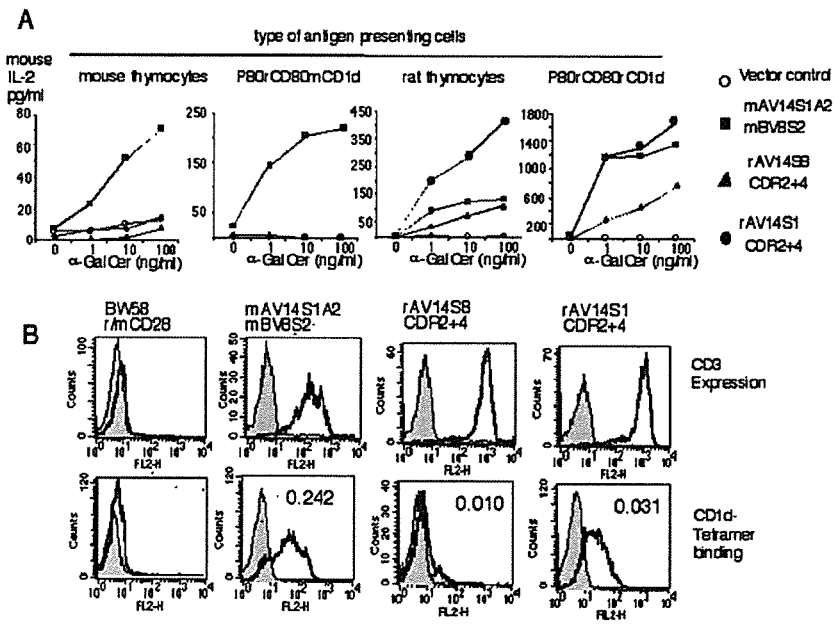

FIGURE 3. *A*, Species specificity of CD1d-restricted α-GalCer recognition by rat iNKT TCR-transduced cells. The graphs in the upper row indicate degree of IL-2 production (please note the different scales of the ordinates) by TCR-transduced BW58r/mCD28 cells after stimulation with α-GalCer presented by different APC-expressing mouse or rat CD1d. Transduced TCR: ○, vector control; ■, mAV14S1A2+mBV8S2 (mouse α-chain + mouse β-chain); ▲, AV14S8 + rat CDR2+4 β-chain (rat AVS8 α-chain + BV8S4-like rat β-chain); ●, AV14S1 + rat CDR2+4 β-chain (rat AVS1 α-chain + BV8S4-like rat β-chain). Amino acid sequences of the TCR chains used by these are given in Fig. 2. The type of α-GalCer-presenting cells and concentrations of α-GalCer used for stimulation are indicated on top of the respective graphs and at the abscissa, respectively. Zero ng/ml indicates the use of vehicle control. *B, Upper row*, CD3 expression of TCR-transduced cell lines used in *A*. Binding of isotype control (▨) or anti-CD3 (□). *Lower row*, Mouse CD1d tetramer staining. Binding of unloaded control (350 ng/50 μl sample, ▨) and of α-GalCer-loaded tetramers (350 ng/50-μl sample, □). The type of transduced TCR is given on top of the histograms. The numbers in the histogram give ratios of MFIs for staining with α-GalCer-loaded mouse CD1d tetramers divided by that for staining with anti-CD3.

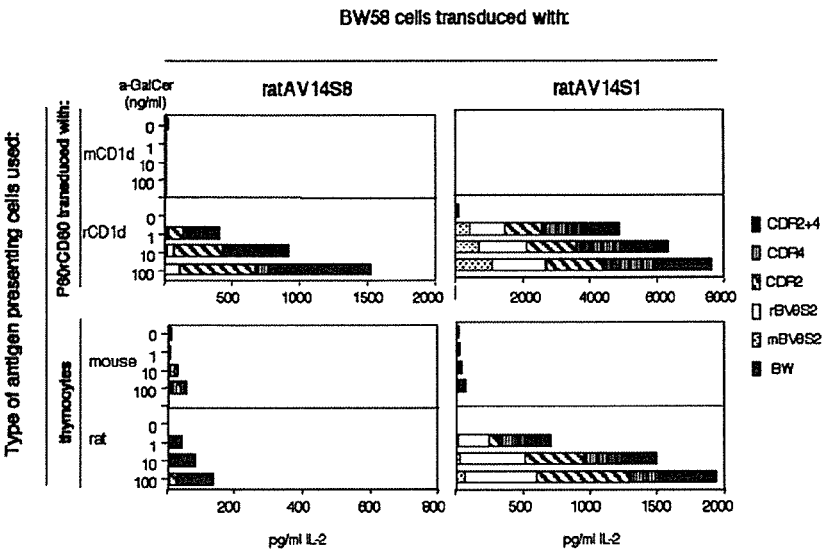

FIGURE 4. CD1d-restricted α-GalCer recognition of rat iNKT TCR. Species specificity of CD1d restriction. Shown is the α-GalCer-induced IL-2 production of BW58r/m CD28 transduced with rat AV14S1 or AV148 α-chains and various β-chains and different types of APC. Each section of the column indicates IL-2 production by cells expressing a certain α-β-chain combination. The α-chain is indicated at the top of the graph, the β-chains are indicated by the symbols in the graph. BW, Cells transduced with vector control. Ordinate, Type of APCs and the origin of CD1d. Note the variation of the scales indicating IL-2 production in the various graphs. α-GalCer concentrations are given in nanograms per milliliter. Vehicle designates culture with solvent (DMSO) only.

Effects of iNKT TCR α- and β-chain differences on CD1d-restricted α-GalCer recognition

We have previously analyzed the effects of CDR2 and/or CDR4 mutations of rat BV8S2 on the recognition of peptide Ags and superantigens (33). To learn whether the known BV encoded (super)Ag recognition sites may also contribute to α-GalCer recognition, AV14 α-chains were coexpressed with the various rat BV8S2 β-chain mutants and a mouse BV8S2 β-chain. These lines were then tested for the response to α-GalCer presented either by rat or mouse CD1d and for binding of α-GalCer-loaded mouse CD1d tetramer.

All lines expressed similar levels of TCR (summarized in Fig. 6) and produced similar amounts of IL-2 after stimulation with anti-CD3 mAb, with the exception of the mouse β-chain-expressing lines, which sometimes showed a rather low level of IL-2 production (data not shown). All lines were tested two to five times; and although the overall degree of stimulation varied between experiments, the patterns of α-GalCer reactivity remained the same. Figs. 4 and 5 show results from a representative experiment comparing all cell lines and Fig. 6 summarizes the results of all experiments.

The iNKT TCR composition affected the α-GalCer reactivity as follows: 1) the α-chain sequence of the transduced TCR largely affected the general degree of α-GalCer reactivity, because all rat AV14S1 α-chain-expressing lines responded considerably better to α-GalCer than the corresponding rat AV14S8 α-chain-expressing lines (Figs. 3 and 4); 2) lines with TCR comprising the two rat α-chains showed no or only a marginal response to α-GalCer which was presented by mouse CD1d, regardless of the type of the pairing β-chain (Fig. 4). These findings confirmed and extended the results on the species specificity of CD1d-restricted α-GalCer recognition by rat iNKT TCR shown in Fig. 3) only lines with TCR comprising the mouse α-chain in combination with mouse β-chain or with suitable rat β-chains responded to α-GalCer presented by mouse CD1d (Fig. 5). Suitable were those rat β-chains, which contained the BV8S4-like CDR2 (CDR2 or CDR2+4 mutant), whereas β-chains with the CDR2 of rat BV8S2 (CDR4 mutant and wild-type BV8S2) showed in the same setting only a marginal or no response. This pattern of reactivity maps the CDR2 of the β-chain as a region contributing to CD1d-restricted α-GalCer recognition in the interspecies comparison.

In contrast to the variation in the response to α-GalCer presented by mouse CD1d, recognition of rat CD1d-α-GalCer complexes was largely unaffected by the β-chain of iNKT TCR. All lines expressing TCR comprising the rat or mouse AV14S1 α-chains (Figs. 4 and 5) showed a very similar response. The

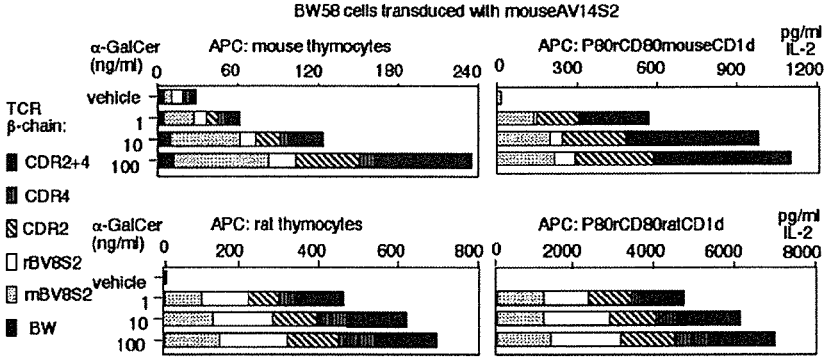

FIGURE 5. Analysis of mouse CD1d restricted α -GalCer recognition by chimeric mouse α- rat-β-chain iNKT TCR reveals contribution of CDR2β to ligand recognition by iNKT TCR. Shown is IL-2 production of BW58r/m CD28 transduced with AV14S1A2 α-chains and various β-chains indicated by the symbols in the graph to α-GalCer presented by indicated APC. BW indicates cells transduced with vector control. Every section of the columns indicates IL-2 production by cells expressing a certain α-β-chain combination. Note the variation of the scales indicating IL-2 production in the various graphs. α-GalCer concentrations are given in ng/ml. Vehicle designates culture with solvent (DMSO) only.

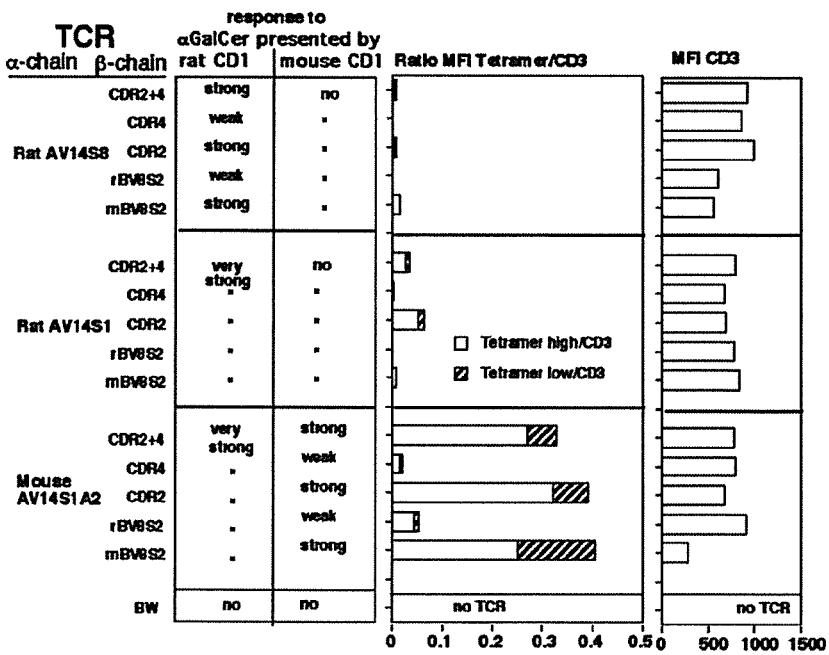

FIGURE 6. Survey of α-GalCer responsiveness of TCR-transduced cell lines, their CD1d tetramer binding, and TCR expression. The left part of the figure summarizes functional data of three to five experiments on the response to α-GalCer presented by rat or mouse CD1d by cell lines expressing the indicated iNKT TCR combinations (see also Figs. 3–5). The central part gives an estimate on CD1d tetramer binding for different cell lines. The stacked bars depict the ratio of MFIs obtained by staining with 350 ng (tetramer high) or 35 ng (tetramer low) of CD1d tetramer divided by the MFI of anti-CD3 staining. Numbers on the abscissa indicate this ratio. Examples for the staining are given in Fig. 3. The right part gives the MFI of CD3 staining of the cell lines used to generate of the data depicted in the central part of the graph.

somewhat lower IL-2 production of the line coexpressing rat AV14S1 α-chain and the CDR4 mutant β-chain probably reflects a generally weaker capacity in TCR-triggered IL-2 production, because anti-CD3 induced IL-2 secretion (not shown) was only about one-half of that found for the other lines. Less clear were the results for cell lines expressing rat AV14S8 α-chain. In two of four experiments, β-chain composition affected the response to rat CD1-α-GalCer complexes of the lines. An example for such a differential response is given in Fig. 4, where the lines expressing the CDR2 or CDR2+4 mutant β-chains reacted far better than those lines expressing the wild-type BV8S2 or the CDR4 mutant.

Finally, effects of the α-chain composition were also seen for the three mouse β-chain-expressing lines. The rat AV14S8 α-chain/mouse β-chain-expressing line completely lacked α-GalCer reactivity (Fig. 4), whereas the rat AV14S1 α-chain/mouse β-chain expressing line responded to α-GalCer if it was presented by rat CD1d-transduced P80rCD80 cells (Fig. 4), implicating rat Vα interactions with CD1d in imparting the observed species specificity. Only the mouse AV14S1A2 α-chain/mouse β-chain expressing line responded irrespective of the types of APC or origin of CD1d used to present the α-GalCer (Fig. 4).

Differential binding of α-GalCer-loaded mouse CD1d tetramers to iNKT-TCR-transduced lines

All cell lines were also tested for TCR expression and binding of α-GalCer-loaded tetramers at two different concentrations. In all cases, binding of unloaded tetramer control was negligible. Fig. 6 summarizes data from such an experiment and gives an overview of the results obtained in the functional assays. The capacity to bind α-GalCer-loaded mouse CD1d tetramers is presented by the ratio of MFI of tetramer binding and MFI of anti-CD3 binding. The best binding was found for the TCR comprising mouse AV14S1 α-chain paired with the CDR2, CDR2+4 mutants of rat BV8S2 β-chains or the mouse BV8S2 β-chain (Figs. 3 and 6), which is consistent with their exclusive capacity to respond to α-GalCer presented by mouse CD1d. At least 8 times weaker was the tetramer binding of lines coexpressing mouse α-chains and rat BV8S2 and CDR4 mutants.

Interestingly, the tetramer binding varied also between the rat α-chain-expressing lines. The poorly responding rat AV14S8 α-chain-expressing lines showed essentially no binding, whereas at least some tetramer binding was found for the more reactive lines coexpressing rat AV14S1 α-chain and the suitable CDR2 or CDR2+4 mutated β-chains. Finally, and again consistent with the functional assays, the rat α-chains paired with mouse β-chain bound no tetramer, whereas the original mouse iNKT TCR bound it very well. Indeed, the efficient binding of this TCR at the lower tetramer concentration suggests a rather high avidity of the original mouse iNKT TCR for α-GalCer-mouse CD1d complexes, consistent with measurements conducted with other mouse iNKT cell hybridomas and T cell populations.

Fig. 6 summarizes our results on the CD1d-restricted α-GalCer response and binding of α-GalCer-loaded mouse CD1d tetramers to iNKT TCR-transduced cell lines. It appears that the lack of reactivity to α-GalCer presented by mouse CD1d results from an impaired binding of the rat iNKT TCR α- rather than β-chain to mouse CD1d. Furthermore, comparison of iNKT TCR sharing the same α-chain but comprising different β-chains revealed that the amino acid composition of CDR2 of the β-chain strongly affects the CD1d-restricted glycolipid reactivity.

Discussion

This study was initiated to characterize the phenotype and the α-GalCer response of rat iNKT cells in a side by side comparison of mouse and rat IHL. As previously described (1, 6, 28), ~30% of mouse IHL coexpressed NK1.1 and TCR and were either $CD4^+$ or $CD4^-CD8^-$, whereas rat IHL comprised rather low numbers of NKR-P1A (rat homolog of NK1.1) and TCR^+ cells, most of them being $CD8\alpha\beta^+$. Our attempts to directly detect rat iNKT cells by staining with α-GalCer-loaded mouse CD1d tetramers failed, although the capacity of rat IHL to produce IFN-γ and IL-4 production after stimulation with α-GalCer suggested that there is indeed a functional iNKT cell population in F344/Crl rats. Analysis of newly generated cell lines expressing CD1d and iNKT TCR of both species allowed us to directly demonstrate the functionality of the rat elements of cognate Ag recognition by iNKT cells. In

addition, this analysis revealed that Ag recognition by rat iNKT TCR required its presentation by syngeneic CD1d, which was unexpected, given that mouse and human CD1d tetramers and dimers (18–20) bind to iNKT cells of the opposite species. Nevertheless, despite this cross-species reactivity, mouse iNKT TCRs bind mouse CD1d better than human CD1d, as was shown with α-GalCer-loaded mouse CD1d dimers (4). In addition, the weakly binding human dimers showed a stronger preference for mouse BV8S2 iNKT TCR than for mouse dimers, a result that underlines the substantial contribution of the β-chain to binding of α-GalCer CD1d complexes (4).

Interestingly, mouse iNKT TCR-transduced lines responded quite well to α-GalCer presented by rat and by mouse CD1d, whereas the rat iNKT TCR-expressing lines responded only when Ag was presented by rat CD1d. What could be the reason for the need of syngenicity between iNKT TCR and CD1d only in one direction? One possibility could be that higher numbers of α-GalCer complexes on rat $CD1d^+$ APCs could have compensated for the generally low avidity of rat iNKT TCR for CD1d, in particular for mouse CD1d. This possibility cannot be formally excluded but seems to be rather unlikely because homologous types of APC were used for presentation. Alternatively, we suggest a higher degree of promiscuity either in Ag recognition by mouse vs rat iNKT TCR or in Ag presentation by rat vs mouse CD1d.

With the help of chimeric and mutated iNKT TCR, we could identify TCR regions, which contribute to binding of α-GalCer and (mouse) CD1d. Cell lines expressing TCR comprising a mouse iNKT TCR α-chain and a suitable β-chain transgressed the threshold for the induction of a response to Ags presented by mouse CD1d, and these cells efficiently bound mouse CD1d tetramers. The differential reactivity of the rat BV8S2 β-chain mutants allowed us for the first time to demonstrate the important role of BV-encoded parts in the α-GalCer response, without a possible interference by CDR3 diversity. In addition, analysis of mutants swapping the CDR2 of BV8S2 with that of BV8S4 provided evidence for an involvement of the CDR2 of the β-chain in recognition of the α-GalCer-CD1d complex. In this context, it is of interest that the CDR2 of rat BV8S4, which in the combination with the mouse iNKT TCR α-chain permitted binding of α-GalCer-mouse CD1d complexes, and the CDR2 of mouse BV8S differ from each other by only one amino acid (Fig. 2). In contrast, the CDR2 of rat BV8S2, which in the interspecies comparison was nonpermissive, differed from that of mouse BV8S2 by 3 aa.

Rat *Tcrb* haplotypes vary in expression of functional BV8S2 and BV8S4 genes. The $Tcrb^a$ haplotype, which is found in F344/Crl and DA rats, expresses BV8S2 and BV8S4, whereas the $Tcrb^l$ haplotype of LEW/Cr, BN, and PVG rats expresses only BV8S2 (24, 31, 41, 42). These rat strains are widely used as models for autoimmune diseases; therefore, it is of special interest to investigate whether differences in reactivity to natural iNKT TCR ligands based on differences in the CDR2s of BV8S2 vs BV8S4 could lead to a rat strain-specific variation in iNKT T cell development or Ag reactivity.

The three α-chains tested contributed not only to restricted recognition of syngeneic CD1d, but also to the overall magnitude of the α-GalCer response. The lines expressing TCR with rat AV14S1 chains and mouse AV14S1A2 α-chains showed a much better response than the rat AV14S8-expressing lines. By analogy to what is known from MHC-restricted recognition of peptide Ags, the differences in α-GalCer reactivity of the two rat α-chains could have been explained by the K50T substitution in the CDR2α and by the A93V difference in the CDR3α (43). Two reasons lead us to assume that the CDR2α difference is of minor importance. In a comprehensive study on a mouse AV14S1 polymorphism, Sim et al. (44) demonstrated that a pronounced CDR2α difference between mouse AV14S1A1 and AV14S1A2 (see also Fig. 2) had little if any effect on TCR-binding to α-GalCer-CD1d complexes (44). Also, our own preliminary results (E. Pyz, I. Müller, and T. Herrmann, unpublished observations) obtained with rat AV14S1 and AV14S8 chain mutants showed little effect of the K50T substitution on the α-GalCer response, whereas a pronounced effect was found for the V93A substitution.

To sum up, we showed that efficient activation of rat iNKT TCR-expressing lines requires presentation of α-GalCer by syngeneic CD1d, and that reactivity to complexes of α-GalCer and mouse CD1d can be obtained by replacing the rat α-chain against that of the mouse and by using a β-chain comprising the CDR2 of rat BV8S4.

This finding thus provides the first description of a germline-encoded CDR involved in ligand recognition by iNKT TCR. The generation and functional analysis of further chimeric rat/mouse iNKT TCR and of chimeric rat/mouse CD1d molecules should strongly facilitate the characterization of the TCR/CD1d/Ag complex. At a certain point of chimerism of TCR or CD1d, cells expressing iNKT TCR comprising rat/mouse α-chain chimeras would be expected to gain specificity for α-GalCer presented by mouse CD1d and mouse/rat CD1d chimeras should gain the capacity to efficiently present Ag to rat iNKT TCR. Finally, combined functional assays with cells expressing such chimeric or mutated receptors and ligands, at best together with binding studies of recombinant molecules, may even allow definition of direct contacts in the ternary complex comprising iNKT TCR/Ag and CD1d.

Acknowledgments

We thank Kathrin Krejci and Ingrid Müller for excellent technical assistance and Niklas Beyersdorf and Barabara Sullivan for critical reading of the manuscript.

Disclosures

The authors have no financial conflict of interest.

References

1. Godfrey, D. I., H. R. MacDonald, M. Kronenberg, M. J. Smyth, and L. Van Kaer. 2004. NKT cells: what's in a name? *Nat. Rev. Immunol.* 4: 231–237.
2. Lantz, O., and A. Bendelac. 1994. An invariant T cell receptor α chain is used by a unique subset of major histocompatibility complex class I-specific $CD4^+$ and $CD4^-8^-$ T cells in mice and humans. *J. Exp. Med.* 180: 1097–1106.
3. Matsuda, J. L., L. Gapin, N. Fazilleau, K. Warren, O. V. Naidenko, and M. Kronenberg. 2001. Natural killer T cells reactive to a single glycolipid exhibit a highly diverse T cell receptor β repertoire and small clone size. *Proc. Natl. Acad. Sci. USA* 98: 12636–12641.
4. Schumann, J., R. B. Voyle, B. Y. Wei, and H. R. MacDonald. 2003. Cutting edge: influence of the TCR Vβ domain on the avidity of CD1d:α-galactosylceramide binding by invariant Vα14 NKT cells. *J. Immunol.* 170: 5815–5819.
5. Dellabona, P., E. Padovan, G. Casorati, M. Brockhaus, and A. Lanzavecchia. 1994. An invariant Vα24-JαQ/Vβ 11 T cell receptor is expressed in all individuals by clonally expanded $CD4^-8^-$ T cells. *J. Exp. Med.* 180: 1171–1176.
6. Matsuura, A., M. Kinebuchi, H. Z. Chen, S. Katabami, T. Shimizu, Y. Hashimoto, K. Kikuchi, and N. Sato. 2000. NKT cells in the rat: organ-specific distribution of NKT cells expressing distinct Vα14 chains. *J. Immunol.* 164: 3140–3148.
7. Swann, J., N. Y. Crowe, Y. Hayakawa, D. I. Godfrey, and M. J. Smyth. 2004. Regulation of antitumour immunity by CD1d-restricted NKT cells. *Immunol. Cell Biol.* 82: 323–331.
8. Skold, M., and S. M. Behar. 2003. Role of CD1d-restricted NKT cells in microbial immunity. *Infect. Immun.* 71: 5447–5455.
9. Taniguchi, M., M. Harada, S. Kojo, T. Nakayama, and H. Wakao. 2003. The regulatory role of Vα14 NKT cells in innate and acquired immune response. *Annu. Rev. Immunol.* 21: 483–513.
10. Giabbai, B., S. Sidobre, M. D. Crispin, Y. Sanchez-Ruiz, A. Bachi, M. Kronenberg, I. A. Wilson, and M. Degano. 2005. Crystal structure of mouse CD1d bound to the self ligand phosphatidylcholine: a molecular basis for NKT cell activation. *J. Immunol.* 175: 977–984.
11. Koch, M., V. S. Stronge, D. Shepherd, S. D. Gadola, B. Mathew, G. Ritter, A. R. Fersht, G. S. Besra, R. R. Schmidt, E. Y. Jones, and V. Cerundolo. 2005. The crystal structure of human CD1d with and without α-galactosylceramide. *Nat. Immunol.* 6: 819–826.

12. Zajonc, D. M., C. Cantu, 3rd, J. Mattner, D. Zhou, P. B. Savage, A. Bendelac, I. A. Wilson, and L. Teyton. 2005. Structure and function of a potent agonist for the semi-invariant natural killer T cell receptor. *Nat. Immunol.* 6: 810–818.
13. Zhou, D., J. Mattner, C. Cantu III, N. Schrantz, N. Yin, Y. Gao, Y. Sagiv, K. Hudspeth, Y. Wu, T. Yamashita, et al. 2004. Lysosomal glycosphingolipid recognition by NKT cells. *Science* 306: 1786–1789.
14. Kinjo, Y., D. Wu, G. Kim, G. W. Xing, M. A. Poles, D. D. Ho, M. Tsuji, K. Kawahara, C. H. Wong, and M. Kronenberg. 2005. Recognition of bacterial glycosphingolipids by natural killer T cells. *Nature* 434: 520–525.
15. Mattner, J., K. L. Debord, N. Ismail, R. D. Goff, C. Cantu, 3rd, D. Zhou, P. Saint-Mezard, V. Wang, Y. Gao, N. Yin, et al. 2005. Exogenous and endogenous glycolipid antigens activate NKT cells during microbial infections. *Nature* 434: 525–529.
16. Sandberg, J. K., and H. G. Ljunggren. 2005. Development and function of CD1d-restricted NKT cells: influence of sphingolipids, SAP and sex. *Trends Immunol.* 26: 347–349.
17. MacDonald, H. R. 2000. CD1d-glycolipid tetramers: A new tool to monitor natural killer T cells in health and disease. *J. Exp. Med.* 192: F15–F20.
18. Matsuda, J. L., O. V. Naidenko, L. Gapin, T. Nakayama, M. Taniguchi, C. R. Wang, Y. Koezuka, and M. Kronenberg. 2000. Tracking the response of natural killer T cells to a glycolipid antigen using CD1d tetramers. *J. Exp. Med.* 192: 741–754.
19. Karadimitris, A., S. Gadola, M. Altamirano, D. Brown, A. Woolfson, P. Klenerman, J. L. Chen, Y. Koezuka, I. A. Roberts, D. A. Price, et al. 2001. Human CD1d-glycolipid tetramers generated by in vitro oxidative refolding chromatography. *Proc. Natl. Acad. Sci. USA* 98: 3294–3298.
20. Benlagha, K., A. Weiss, A. Beavis, L. Teyton, and A. Bendelac. 2000. In vivo identification of glycolipid antigen-specific T cells using fluorescent CD1d tetramers. *J. Exp. Med.* 191: 1895–1903.
21. Naidenko, O. V., J. K. Maher, W. A. Ernst, T. Sakai, R. L. Modlin, and M. Kronenberg. 1999. Binding and antigen presentation of ceramide-containing glycolipids by soluble mouse and human CD1d molecules. *J. Exp. Med.* 190: 1069–1080.
22. Ichimiya, S., K. Kikuchi, and A. Matsuura. 1994. Structural analysis of the rat homologue of CD1: evidence for evolutionary conservation of the CD1D class and widespread transcription by rat cells. *J. Immunol.* 153: 1112–1123.
23. Katabami, S., A. Matsuura, H. Z. Chen, K. Imai, and K. Kikuchi. 1998. Structural organization of rat CD1 typifies evolutionarily conserved CD1D class genes. *Immunogenetics* 48: 22–31.
24. Asmuss, A., K. Hofmann, T. Hochgrebe, G. Giegerich, T. Hunig, and T. Herrmann. 1996. Alleles of highly homologous rat T cell receptor β-chain variable segments 8.2 and 8.4: strain-specific expression, reactivity to superantigens, and binding of the mAb R78. *J. Immunol.* 157: 4436–4441.
25. Kinebuchi, M., and A. Matsuura. 2004. Rat T-cell receptor TRAV11 (Vα14) genes: further evidence of extensive multiplicity with homogeneous CDR1 and diversified CDR2 by genomic contig and cDNA analysis. *Immunogenetics* 55: 756–762.
26. Shimamura, M., J. Miura-Ohnuma, and Y. Y. Huang. 2001. Major sites for the differentiation of Vα14$^+$ NKT cells inferred from the V-J junctional sequences of the invariant T-cell receptor α chain. *Eur J. Biochem.* 268: 56–61.
27. Brissette-Storkus, C., C. L. Kaufman, L. Pasewicz, H. M. Worsey, R. Lakomy, S. T. Ildstad, and W. H. Chambers. 1994. Characterization and function of the NKR-P1dim/T cell receptor-$\alpha\beta^+$ subset of rat T cells. *J. Immunol.* 152: 388–396.
28. Badovinac, V., C. Boggiano, V. Trajkovic, A. B. Frey, N. L. Vujanovic, D. P. Gold, M. Mostarica-Stojkovic, and S. Vukmanovic. 1998. Rat NKR-P1$^+$CD3$^+$ T cells: selective proliferation in interleukin-2, diverse T-cell-receptor-Vβ repertoire and polarized interferon-γ expression. *Immunology* 95: 117–125.
29. Kinebuchi, M., A. Matsuura, K. Ohya, W. Abo, and J. Kitazawa. 2005. Contribution of Vα24Vβ11 natural killer T cells in Wilsonian hepatitis. *Clin. Exp. Immunol.* 139: 144–151.
30. Knudsen, E., T. Seierstad, J. T. Vaage, C. Naper, H. B. Benestad, B. Rolstad, and A. A. Maghazachi. 1997. Cloning, functional activities and in vivo tissue distribution of rat NKR-P1$^+$ TCR$\alpha\beta^+$ cells. *Int. Immunol.* 9: 1043–1051.
31. Herrmann, T., K. Hofmann, N. E. Nagel, A. Asmuss, T. Hunig, and K. Wonigeit. 1999. Differential CD4/CD8 subset-specific expression of highly homologous rat Tcrb-V8 family members suggests a role of CDR2 and/or CDR4 (HV4) in MHC class-specific thymic selection. *Int. Immunol.* 11: 435–444.
32. Emoto, M., Y. Emoto, and S. H. Kaufmann. 1995. IL-4 producing CD4$^+$ TCR $\alpha\beta$ in liver lymphocytes: influence of thymus, β_2-microglobulin and NK1.1 expression. *Int. Immunol.* 7: 1729–1739.
33. Kreiss, M., A. Asmuss, K. Krejci, D. Lindemann, T. Miyoshi-Akiyama, T. Uchiyama, L. Rink, C. P. Broeren, and T. Herrmann. 2004. Contrasting contributions of complementarity-determining region 2 and hypervariable region 4 of rat BV8S2$^+$ (Vβ8.2) TCR to the recognition of myelin basic protein and different types of bacterial superantigens. *Int. Immunol.* 16: 655–663.
34. Makowska, A., T. Kawano, M. Taniguchi, and S. Cardell. 2000. Differences in the ligand specificity between CD1d-restricted T cells with limited and diverse T-cell receptor repertoire. *Scand. J. Immunol.* 52: 71–79.
35. Kuss, A. W., M. Knodel, F. Berberich-Siebelt, D. Lindemann, A. Schimpl, and I. Berberich. 1999. A1 expression is stimulated by CD40 in B cells and rescues WEHI 231 cells from anti-IgM-induced cell death. *Eur. J. Immunol.* 29: 3077–3088.
36. Luhder, F., Y. Huang, K. M. Dennehy, C. Guntermann, I. Muller, E. Winkler, T. Kerkau, S. Ikemizu, S. J. Davis, T. Hanke, and T. Hunig. 2003. Topological requirements and signaling properties of T cell-activating, anti-CD28 antibody superagonists. *J. Exp. Med.* 197: 955–966.
37. Maeda, K., T. Sato, M. Azuma, H. Yagita, and K. Okumura. 1997. Characterization of rat CD80 and CD86 by molecular cloning and mAb. *Int. Immunol.* 9: 993–1000.
38. Teitell, M., H. R. Holcombe, L. Brossay, A. Hagenbaugh, M. J. Jackson, L. Pond, S. P. Balk, C. Terhorst, P. A. Peterson, and M. Kronenberg. 1997. Nonclassical behavior of the mouse CD1 class I-like molecule. *J. Immunol.* 158: 2143–2149.
39. Bradbury, A., K. T. Belt, T. M. Neri, C. Milstein, and F. Calabi. 1988. Mouse CD1 is distinct from and co-exists with TL in the same thymus. *EMBO J.* 7: 3081–3086.
40. Morita, M., K. Motoki, K. Akimoto, T. Natori, T. Sakai, E. Sawa, K. Yamaji, Y. Koezuka, E. Kobayashi, and H. Fukushima. 1995. Structure-activity relationship of α-galactosylceramides against B16-bearing mice. *J. Med. Chem.* 38: 2176–2187.
41. Torres-Nagel, N. E., T. Herrmann, G. Giegerich, K. Wonigeit, and T. Hunig. 1994. Preferential TCR V usage in rat repertoire selection: Vα8 imparts both positive thymic selection by and alloreactivity to RT1f. *Int. Immunol.* 6: 1367–1373.
42. Stienekemeier, M., K. Hofmann, R. Gold, and T. Herrmann. 2000. A polymorphism of the rat T-cell receptor β-chain variable gene 13 (BV13S1) correlates with the frequency of BV13S1-positive CD4 cells. *Immunogenetics* 51: 296–305.
43. Rudolph, M. G., and I. A. Wilson. 2002. The specificity of TCR/pMHC interaction. *Curr. Opin. Immunol.* 14: 52–65.
44. Sim, B. C., K. Holmberg, S. Sidobre, O. Naidenko, N. Niederberger, S. D. Marine, M. Kronenberg, and N. R. Gascoigne. 2003. Surprisingly minor influence of TRAV11 (Vα14) polymorphism on NKT-receptor mCD1/α-galactosylceramide binding kinetics. *Immunogenetics* 54: 874–883.

網羅的遺伝子発現解析による多発性硬化症の病態・薬物反応性

佐藤準一*,**

MSの発症は多数の遺伝因子と環境因子の複雑な相互作用により規定されており，臨床経過・病巣分布・治療反応性・病理学的所見の観点から多様な病態(clinical heterogeneity)を呈する．遺伝子アレイ(DNA microarray/GeneChip)は基盤上に数万遺伝子が貼りつけてあるチップである．遺伝子アレイによるMS患者末梢血リンパ球・脳組織の網羅的遺伝子発現解析は，MS分子遺伝学的発症機序の解明に威力を発揮する．従来の研究方法では予期しなかった遺伝子群のMS病態における重要な役割を発見したり，インターフェロン応答遺伝子群(IFN-responsive genes：IRG)を同定して治療反応性や副作用を事前に予知することが可能になりつつある．最近われわれは階層的クラスター解析(hierarchical clustering analysis)により，MSがT細胞の遺伝子発現プロフィールにもとづき4群に分類され，各群は疾患活動性・病変分布・IFN-β治療反応性と密接な対応を認めることを見出した．遺伝子アレイ解析はMSのテーラーメイド医療の樹立に役立つと思われる．

はじめに

多発性硬化症(multiple sclerosis：MS)は中枢神経系白質に炎症性脱髄巣が多発し，さまざまな神経症状が再発をくり返して進行する難病である．MS発症機序は十分解明されていないが，遺伝的要因と環境因子の相互作用を背景に，脳炎惹起性髄鞘抗原に分子相同性を示すウイルスなどの外来抗原を認識し活性化した自己反応性CD4$^+$ Th1 T細胞が，血液脳関門を通過して中枢神経系組織内に浸潤し，マクロファージ・ミクログリアを活性化して腫瘍壊死因子-α(tumor necrosis factor-α：TNF-α)などの炎症増強因子の産生を誘導し脱髄(demyelination)が惹起されると考えられている(自己免疫機序)[1]．回復期には髄鞘再生を認めるが，炎症が遷延化すると髄鞘再生不全・軸索傷害・神経変性をきたして不可逆的機能障害を残す．近年欧米およびわが国における大規模臨床試験により，インターフェロン(IFN)-βのMS再発抑制効果が立証され，現在では急性増悪期に副腎皮質ステロイド短期間大量静脈内投与(intravenous methylpredonisolone pulse：IVMP)をおこない，回復期にIFN-βの継続的皮内・筋肉内投与をおこなう方法が，最も一般的な治療法として選択されている．しかしIFN-βがまったく効果を示さない症例も多い[2]．すなわちMSは均一な疾患ではなく多様な病態を呈する疾患群である可能性が高い．実際MSは臨床経過から再発寛解

〔キーワード〕
DNAマイクロアレイ
遺伝子発現プロフィール
階層的クラスター解析
多発性硬化症
テーラーメイド医療

*SATOH Jun-ichi/国立精神・神経センター神経研究所免疫研究部
**明治薬科大学薬学部生命創薬科学科生命情報解析学

型(relapsing-remitting MS：RRMS)，二次進行型(secondary-progressive MS：SPMS)，一次進行型(primary-progressive MS：PPMS)，病巣分布から脳型(conventional MS：CMS)，視神経脊髄型(opticospinal MS：OSMS)，IFN-β治療反応性からレスポンダー(応答)(responder MS：RMS)，ノンレスポンダー(非応答)(nonresponder MS：NRMS)に分類される．病理学的にはT細胞浸潤，抗体沈着，オリゴデンドログリアのアポトーシス(apoptosis)の所見により4型に分類される[3]．

近年MSの免疫病態の多様性(heterogeneity)を解析する手段として遺伝子アレイ(DNA microarray/GeneChip)が用いられている．ヒトゲノムプロジェクトによりヒト全遺伝子塩基配列が解明され，遺伝子アレイを用いて個々の細胞における数万遺伝子(ヒト全遺伝子約30,000)の発現情報を包括的・網羅的・系統的に解析することが可能になった．RNA発現解析をトランスクリプトーム解析，蛋白質発現解析をプロテオーム解析とよぶ．このような網羅的発現解析(global expression analysis)により，従来の研究方法では予期し得なかった遺伝子群のMS病態における役割がつぎつぎ明らかにされた[4]．また治療に反応する遺伝子群の変動を経時的に解析することにより，薬物反応性や副作用を予知することが可能になりつつある(薬理ゲノミクス，pharmacogenomics)．本稿ではDNAマイクロアレイによるMSの免疫病態・薬物反応性の解析に関する最近の知見を概説する．

1．マイクロアレイ解析の基本原理

遺伝子アレイはスライドグラスやナイロン膜などの基盤上に，数千～一万のcDNAまたはオリゴヌクレオチドが貼りつけてあるチップである．cDNAをスポッターで基盤上にスポットしてあるDNAマイクロアレイと，基盤上で直接高密度オリゴヌクレオチドをフォトリソグラフ合成しているGeneChip(Affymetrix)に分類される．スライドグラスをマイクロアレイ，ナイロン膜をマクロアレイと総称する．まず遺伝子発現レベルが異なる2種類以上の細胞・組織，たとえばIFN-β投与前後の細胞などからmRNAを抽出し増幅する．DNAマイクロアレイでは別々の蛍光色素(Cy 3, Cy 5)で標識したcDNAまたはcRNAを作成して同一チップ上で競合的ハイブリダイゼーションをおこなう(2色法)．GeneChipでは*in vitro* transcriptionによりcDNAからbiotin標識cRNAを作成，断片的に切断してハイブリダイゼーションをおこない，streptoavidin-phycoerythrin(SAPE)を添加して蛍光標識する(1色法)．GeneChipは1サンプルに1枚のアレイが必要でアレイ間の比較になる．どちらの場合もスキャナーで蛍光シグナルを検出，得られたデータを正規化(normalization)し，統計学的解析(R解析：www.cran.r-project.orgなど)をおこない，サンプル間の遺伝子発現プロフィール(gene expression profile)を比較する．したがってRNAの質(quality)が結果に非常に影響する．有意な発現差異を示す遺伝子はリアルタイムRT-PCRで定量・検証することが重要である(validation)．同定した遺伝子の機能・構造に関する情報(annotation)は，Web上でデーターベース(NCBI Entrez：www.ncbi.nlm.nih.gov/Entrez/index.htmなど)を検索する．すでにさまざまな遺伝子発現データがGene Expression Omnibus(GEO：www.ncbi.nlm.nih.gov/geo)に登録されておりダウンロードできる．末梢血リンパ球(peripheral blood mononuclear cells：PBMC)の遺伝子アレイ解析の問題点は，遺伝子発現レベルが年齢・性・喫煙・飲酒・常用薬・嗜好品・精神的ストレスなどの個人差や採血時刻(日内変動)の影響を受けることである(interindividual and intraindividual variation)[5]．また脳組織の解析では死後脳凍結までに要する時間(RNA degradation time)が問題であり，組織pHが参考になる．

複数サンプルの場合はデータセットの要素特性を抽出し分類するため，解析ソフト(GeneSpring：Silicon Genetics-Agilentなど)を用いて，階層的クラスター解析(hierarchical clustering analysis)をおこなう．すなわちサンプルに関する事前情報なしに，類似発現パターンを呈する遺伝子やサンプルをグループに分類し，樹状図(dendrogram)と発現レベルの二次元マトリックスで表示する(教師なし法：unsupervised method)．またグループを特徴づける指標遺伝子(discriminator genes)を抽出して三次元に投射する主成分解析(principal component analysis：PCA)をおこなう．さらに指標遺伝子抽出に用いたデータをtraining setとして機械学習し，新規データセットにおけるサブグループを高次元空間上で線形判別可能な超平面(hyperplane)を同定するサポートベクターマシン(support vector machine：SVM)解析をおこなう(教師あり法：supervised method)．

2．DNAマイクロアレイによる多発性硬化症の免疫病態の解析(表1)

1）MS脳組織の網羅的遺伝子発現解析

Whitneyら[6][7]は独自のcDNAマイクロアレイを用いてMS急性期炎症性病巣と正常様白質(normal-appearing white matter：NAWM)を比較し，MS病巣におけるインターフェロン制御転写因子(interferon-regulatory factor：IRF)-2，5-lipooxygenase発現上昇を報告した．Chabasら[8]はMS脳cDNAライブラリーの網羅的シークエンス解析によりosteopontin(OPN)発現上昇を認め，ラット実験的自己免疫性脳脊髄炎(experimental autoimmune encephalomyelitis：EAE)モデルの脊髄を用いたカスタムオリゴヌクレオチドマイクロアレイ解析でOPN上昇を確認した．OPN遺伝子欠損マウスはEAE惹起に対して抵抗性を示す[8]．Lockら[9]はGeneChipを用いてMS急性炎症性病巣と慢性非活動性病巣を比較し，前者のG-CSF上昇と後者のIgG Fcレセプター，IgEレセプター，ヒスタミンレセプタータイプ1上昇を報告した．またG-CSF投与でEAE軽症化を認め，イムノグロブリンFcRγ鎖遺伝子欠損マウスではEAE慢性化が抑制されることを報告した[9]．

Myckoら[10]はcDNAマイクロアレイ(Clontech)を用いてSPMS慢性活動性病巣と非活動性病巣，脱髄巣辺縁部と中心部を比較し，活動性病巣辺縁部における免疫応答関連遺伝子群(TNF-αなど)の上昇を報告した．Graumannら[11]はcDNAマクロアレイ(Clontech)を用いてMSのNAWMにおける脳虚血関連遺伝子群(HIF-1αなど)の上昇を見出した．Lindbergら[12]はGeneChipを用いてSPMS活動性病巣でのイムノグロブリン産生亢進を見出した．Tajouriら[13]は独自のcDNAマイクロアレイを用いてSPMS急性・慢性活動性病巣におけるαB-crystallin，SOD 1の上昇を報告した[13]．これら一連のマイクロアレイによるMS脳組織の解析は症例数・サンプル数が少なく，RNA抽出部位が全体像を反映していない可能性が残る．

2）MSとコントロールの末梢血リンパ球の比較解析

Ramanathanら[14]はGeneFilter membrane array(Research Genetics)を用いて，MSと健常人のmonocyte-depleted PBMCを比較し，MSにおけるlymphocyte-specific protein tyrosine kinase(LCK)，IL-7 Rの発現上昇を報告した．LCKはAirlaら[15]のcDNAマクロアレイ(Clontech)解析で，RRMSのPBMCにおいてIVMP治療により低下する遺伝子として報告されている．Bomprezziら[16]は独自のcDNAマイクロアレイを用いて，RRMSと健常人のPBMCで発現差異を呈する53遺伝子を同定した．MSではT細胞活性化関連遺伝子群IL-7 R，ZAP 70，TNFRSF 7(CD 27)の上昇およびサイトカイン

表 1. MS の免疫病態のマイクロアレイ解析

Authors (Reference No.)	Year	No of MS Patients and Controls	RNA Samples	Type of Microarray	No of Genes on Microarray	Key Findings
Whitney *et al*[6]	1999	PPMS(n=1)	acute lesion vs NAWM	Original cDNA Glass Array	1,344 or 5,000	Upregulation of IRF-2 and TNFRp75 in acute lesions
Ramanathan *et al*[14]	2001	RRMS(n=15)vs HC(n=15)	monocyte-depleted PBMC	GeneFilters GF211 Membrane Array(Research Genetics)	5,184	Upregultion of LCK, IL-7R and MMP-19 and downregulation of CCR6 and DFFA in MS
Wandinger *et al*[25]	2001	RRMS(n=1)plus HC(n=2)	PBMC incubated with IFNβ *in vitro*	Mini-Lymphochip cDNA Array	6,432	Upregulation of proinflammatory genes such as CCR5, IP-10, and IL-15RA by IFN-β treatment
Whitney *et al*[7]	2001	PPMS(n=1), RRMS(n=1), EAE vs HC(n=3)	acute or chronic lesions of MS and EAE vs white matter of non-MS controls	Original cDNA Glass Array	2,798	Upregulation of 5-lipoxygenase in MS and EAE lesions
Lock *et al*[9]	2002	CPMS and SPMS(n=4)	acute or chronic active lesions vs chronic silent lesions	HuGene FL Oligonucleotide Array(Affymetrix)	7,026	Upregulation of G-CSF in active lesions and upregulation of IgG FcR in silent lesions, and amelioration of EAE in FcRγ-KO mice and by treatment with G-CSF
Mass *et al*[22]	2002	RA(n=20), SLE(n=24), IDDM(n=5), and MS(n=5)vs HC before and after influenza vaccination(n=9)	PBMC	GeneFilters GF211 Membrane Array(Research Genetics)	4,329	Indistinguishable profiles between MS and IDDM and downregulation of apoptosis-regulatory genes in autoimmune diseases
Bomprezzi *et al*[16]	2003	RRMS(n=18), SPMS(n=6)vs HC(n=21)	PBMC(fresh or frozen)	Original cDNA Array (Modified Lymphochip)	6,500 or 7,500	Upregulation of PAFAH1B1, IL-7R, ZAP70, and TNFRSF7(CD27)and downregulation of HSPA1A (HSP70)and CKS2 in MS
Graumann *et al*[11]	2003	SP/PP/RRMS(n=10)vs non-neurological controls(n=7)	NAWM vs control white matter	Atlas Human cDNA Memebrane Array 1.2 (Clontech)	3,528	Upregulation of ischemic preconditioning genes such as HIF-1α in NAWM of MS
Koike *et al*[26]	2003	RRMS(n=13)before and at 3 and 6 months after IFN-β treatment	T and non-T cells separated from PBMC	Human cDNA Array (Hitachi Life Science)	1,258	Upregulation of 15 IFN-responsive genes in MS after IFN-β treatment
Mycko *et al*[10]	2003	SPMS(n=4)	chronic active vs silent lesions and the lesion margin vs center	Atlas Human 1.0 Glass Microarray(Clontech)	588	Upregulation of inflammation/immune-related genes in the margin of active lesions

Stürzbecher *et al*[34]	2003	RRMS before and after IFN-β treatment for 6 months (n=10, 6 responders vs 4 non-responders)	frozen PBMC *ex vivo* or incubated with IFN-β *in vitro*	Mini-Lymphochip cDNA Array	6,432 or 12,672	Downregulation of IL-8 in responders after IFN-β treatment
Tajouri *et al*[13]	2003	SPMS (n=5) vs non-MS	acute and chronic active lesions	Custom-made cDNA Glass Array	5,000	Upregulation of αB-crystallin and SOD in acute lesions
Weinstock-Guttman *et al*[32]	2003	RRMS before and at 1, 2, 4, 8, 24, 120, and 160h after IFN-β treatment (n=8)	monocyte-depleted PBMC	GeneFilters GF211 Membrane Array (Research Genetics)	5,184	Time-dependent upregulation of IFN-responsive genes
Achiron *et al*[19]	2004	RRMS (n=26, 14 with treatment) vs HC (n=18)	PBMC	Human U95Av2 Oligonucleotide Array (Affymetrix)	12,000	Upregulation of T cell activation genes and downregulation of IL-1 and TNF signaling genes in MS
Achiron *et al*[20]	2004	RRMS treated (n=13) vs untreated (n=13)	PBMC	Human U95Av2 Oligonucleotide Array (Affymetrix)	12,000	Identification of SCYA4, IL2RG, and TNFRSF6 (Fas) as immunomodulatory treatment-associated genes
Airla *et al*[15]	2004	RRMS (n=6) before and after IVMP	PBMC	Atlas Human Hematology/Immunology Membrane Array (Clontech)	448	Downregulation of LCK, TCF7, CD5, and ISGF3 by IVMP
Hong *et al*[35]	2004	RRMS/SPMS treated with IFN-β (n=18), GA (n=12) or untreated (n=15)	PBMC	Original Membrane Array	36	Distinct gene expression profile between MS patients treated with IFN-β and GA
Iglesias *et al*[23]	2004	RRMS (n=17) vs HC (n=7)	PBMC	HuGene FL Oligonucleotide Array (Affymetrix)	6,800	Upregulation of E2F transcription factor pathway genes in MS
Lindberg *et al*[12]	2004	SPMS (n=6) vs non-neurological controls (n=12)	active lesions vs NAWM	Human U95A Oligonucleotide Array (Affymetrix)	12,633	Upregulation of genes related to Ig synthesis in active lesions of MS
Mandel *et al*[21]	2004	RRMS (n=13) vs SLE (n=5) vs HC (n=18)	PBMC	Human U95Av2 Oligonucleotide Array (Affymetrix)	12,000	Downregulation of NR4A1 and NR4A3 as the autoimmunity-specific signature
Mayne *et al*[17]	2004	RRMS (n=21) vs HC (n=19)	$CD4^+$T cells	Immune Membrane Array (National Institute on Aging)	1,152	Upregulation of CYFIP2 in MS
Satoh *et al*[18]	2005	RRMS (n=65) plus SPMS (n=7) vs HC (n=22)	T and non-T cells separated from PBMC	Human cDNA Array (Hitachi Life Science)	1,258	Aberrant expression of apoptosis and DNA damage-regulatory genes in MS

Abbreviations : RRMS : relapsing-remitting MS, SPMS : secondary progressive MS, PPMS : primary progressive MS, CPMS : chronic progressive MS, HC : healthy controls, IDDM : insulin-dependent diabetes mellitus, NAWM : normal appearing white matter, PBMC : peripheral blood mononuclear cells, IFN : interferon, GA : glatiramer acetate, IVMP : intravenous methylprednisolone pulse

mRNAの分解制御因子HSPA 1 A(HSP 70)の低下を認めた．Mayneら[17]はRRMSと健常人の末梢血からCD 4$^+$ T細胞をnegative selectionで分離，cDNA membrane array(NIA)を用いて解析し，MSにおけるcytoplasmic FMR 1 interacting protein 2(CYFIP 2)の上昇を報告した．

われわれ[18]は明確なannotationつき1,259遺伝子を掲載したcDNAマイクロアレイ(Hitachi Life Science)を用いて，72例のIFN-β未治療活動性MS(65 RRMS，7 SPMS)と22名の健常人の末梢血からAutoMACS(Miltenyi Biotec)で分離したCD 3$^+$ T細胞，CD 3$^-$ non-T細胞の遺伝子発現プロフィールを解析した．両群間でT細胞173遺伝子，non-T細胞50遺伝子の発現差異を認めた．上位30遺伝子ではT細胞25遺伝子(NR 4 A 2，TCF 8上昇とMAPK 1，SMARCA 3，HSPA 1 A，TRAIL，TOP 1，CCR 5，BAG 1, DAXX, TSC 22, PARP低下など)，non-T細胞27遺伝子(ICAM 1，CDC 42，RIPK 2，SODD，TOP 2 A上昇とBCL 2，RPA 1，NFATC 3, HSPA 1 L, RBBP 4, PRKDC低下など)がアポトーシス制御遺伝子の範疇に属していた．MSでアポトーシス促進遺伝子(proapoptotic genes)と抑制遺伝子(antiapoptotic genes)の発現上昇・低下(拮抗的バランスcounterbalance)を認め，MSにおけるアポトーシス制御異常の存在が示唆された．

Achironら[19]はGeneChipを用いて26例のRRMSと18名の健常人でPBMCの遺伝子発現プロフィールを比較解析した．両群間で1,109遺伝子の発現差異を認め，MSでT細胞活性化関連遺伝子群(LEF 1，TCF 3，SLAM，ITGB 2，CTSB)上昇とIL-1β/TNF-αシグナル伝達系遺伝子群の低下を認めた．われわれの結果[18]に反してMSにおけるorphan nuclear receptor NR 4 A 2の低下を報告した．しかし彼らの研究ではMS 14例は採血時に治療薬IFN-β，glatiramer acetate(GA)，intravenous immunoglobulins(IVIg)を投与中で，遺伝子発現に影響した可能性がある．Achironら[20]は上記の症例を治療群13例と未治療群13例に分けて比較し，治療関連7遺伝子群(TNFRSF 6，Fasなど)を同定した．また13例のRRMSと5例のSLEを18名の健常人と比較し，自己免疫特異的プロフィール(autoimmunity-specific signature)としてアポトーシス制御遺伝子群の発現異常を報告した[21]．Maasら[22]は20例のRA，24例のSLE，5例のIDDM，5例のMS，9名のインフルエンザワクチン接種前後の健常人のPBMCを解析した．ワクチン免疫応答と自己免疫疾患の遺伝子発現パターンはまったく異なるが，RAとSLE間，MSとIDDM間はきわめて類似していた．彼らも自己免疫疾患に共通してアポトーシス制御遺伝子群の発現低下を認めた．Iglesiasら[23]はGeneChipでRRMSと健常人のPBMCを比較解析し，MSにおけるE 2 F transcription factor pathway遺伝子上昇を認め，E 2 F 1遺伝子欠損マウスではEAEが軽症化することを報告した．

3) MSにおけるIFN-β治療反応性の解析

われわれ[24]はcDNAマクロアレイ(Clontech)を用いて，ヒト胎児脳アストロサイト純培養でIFNにより変動する遺伝子を解析し，IFN-βによるIRF-7とpleiotrophinの上昇，IFN-γによるIRF-1とICAM-1の上昇を報告した．Wandingerら[25]はRRMSと健常人のPBMCを*in vitro*でIFN-βにより刺激してcDNAマイクロアレイ(Mini-Lymphochip)で解析し，CC chemokine receptor 5(CCR 5)とinterferon-inducible cytokine IP-10(CXCL 10)の上昇を認めた．われわれ[26]は1,259遺伝子cDNAマイクロアレイ(Hitachi)を用いて，13例のRRMSでIFN-β治療開始前後に採血し，末梢血CD 3$^+$ T細胞とCD 3$^-$ non-T細胞で発現変動した遺伝子群(IFN-responsive genes：IRG)を同定した．T細胞で8遺伝子(IRF-7，ISG 15，IFI 56，IFI 6-

16, IFI 60, IFI 30, ATF 3, TLR 5)の上昇とIL-3, monokine induced by IFN-γ(MIG)の低下, non-T細胞で12遺伝子(IRF-7, ISG 15, IFI 56, IFI 6-16, IFI 27, IFI 17, TAP 1, TNFAIP 6, TSC 22, SULT 1C1, RPC 39, RAB 11 A)の上昇, IL-3の低下を認めた. ISG 15, IFI 56, IFI 6-16, IFI 27, TSC 22, SULT 1C1は治療開始後3〜6ヵ月において持続的上昇を認めた. 一方統計学的有意差はなかったが, 治療後にTh 1関連遺伝子CCR 5(T), IFN-γ(T), TNF-α(non-T)の上昇傾向を認めた. この所見はIFN-β治療はMSでは必ずしも明確なTh 2シフトを誘導しないという見解[25]を支持する. 上記の9遺伝子(IRF-7, ISG 15, IFI 56, IFI 6-16, IFI 60, IFI 17, TAP 1, TNFAIP 6, MIG)はプロモータ領域にIFN-stimulated response element(ISRE)やIRF element(IRF-E)が同定されている既知IRGであり, 治療に直接反応し治療効果に深く関与していると考えられる. IRF-7はウイルス感染時にIFN-α/β産生を増幅する正の制御因子である[27]. IFI 30はクラスII MHC拘束性抗原提示の際, はたらくチオール還元酵素で, IFI 30遺伝子欠損マウスでは抗原呈示能低下をきたす[28]. TAP 1はクラスI MHC拘束性抗原提示の際, はたらくペプチド輸送因子で, TAP 1遺伝子欠損マウスではCD 8^+ T細胞を介する結核菌抵抗力が減弱する[29]. TNFAIP 6はTNF-α, IL-1βにより誘導される分泌蛋白質で抗炎症作用を呈する[30]. 以上のようにMSでIFN-βはantiviral and antiinflammatory mediatorsの発現を誘導することが明らかになった. 興味深いことにSLEでは治療の種類にかかわらずPBMCにおけるIRGの発現レベルが高い[31].

Weinstock-Guttmanら[32]はGeneFilter membrane arrayを用いて, IFN-β治療前後の8例のRRMSでmonocyte-depleted PBMCを経時的に解析してIRGを同定した. 多くはわれわれの同定したIRG[26]とオーバーラップしている. Liangら[33]はWeinstock-Guttmanらのデータ[32]を再解析し, IRGはearly-onset(8時間以内), intermediate-onset(24時間), late-onset(48時間)の3群に分類されることを見出した. Stürzebecherら[34]はcDNAマイクロアレイ(Mini-Lymphochip)を用いてIFN-β治療前後の10例のRRMSでPBMCの遺伝子発現プロフィールを解析した(*ex vivo* 解析). 治療前6ヵ月から開始12ヵ月後まで毎月Gd造影MRIを撮影して活動性病巣数を算出, 治療により病巣数が60%以上減少した症例をレスポンダーと定義した. ノンレスポンダー群を当初から効果のみられないnonresponder from initiation of therapy(INR)と, 開始後一定期間は効果を認めたが中和抗体(neutralizing antibody：NAb)の出現に伴い効果が減弱したnonresponder with development of NAb(NAbNR)の2群に分類した. また培養PBMCをIFN-β刺激して*in vitro* 解析もおこなった. レスポンダーで治療後2倍以上変動した遺伝子は*ex vivo* 25遺伝子(IFI 17, OAS, Stat 1上昇とIL-8, CD 69, c-fos, TSC 22低下など)で, このうちIL-8発現低下はレスポンダーの指標となる可能性が示唆された. 一方*in vitro* IRGは87遺伝子で, レスポンダー, ノンレスポンダー間で発現差異を認めなかった. 彼らの結果と反して, われわれ[26]はIFN-β治療後のnon-T細胞におけるTGF-β-stimulated protein TSC 22上昇を報告している. 彼らの研究は症例数が少なく, 凍結保存したPBMCを解凍して用いており, 実験操作で遺伝子発現が変化しうる点が問題である. また1例のレスポンダーでは治療前に約90個のGd造影病巣を呈しているが, これほど多数の造影病巣を示す症例は日本人MSでは異例である. Hongら[35]は主要免疫応答36遺伝子を掲載したcDNAマクロアレイを用いて, 未治療MSとIFN-β, GA治療MSのPBMCを解析し, 治療反応性遺伝子群の相違を明らかにした. 興味深いことに活性化T細胞の血液脳関門通過に重要な

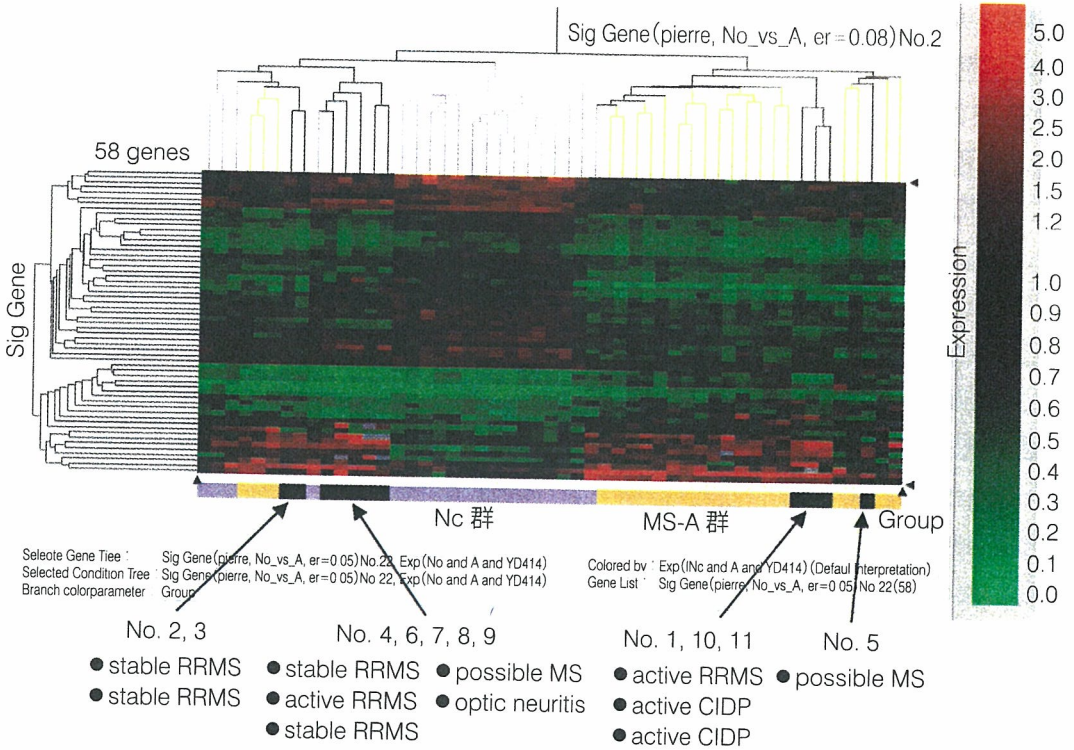

図 1. 階層的クラスター解析

未治療 MS(n=72)と健常人 Nc(n=22)の T 細胞の cDNA マイクロアレイ(1,259 遺伝子)解析で発現差異を認める 286 遺伝子を指標遺伝子(discriminator genes)とする階層的クラスター解析(hierarchical clustering analysis)で，MS 群は Nc 群と分離され A，B，C，D の 4 群に分類された．A 群は遺伝子発現プロフィールが最も Nc 群に類似し，群間検定で両者を識別する 58 遺伝子を抽出した．新規 11 症例(2 例の活動性 MS，4 例の非活動性 MS，2 例の possible MS，1 例の視神経炎，2 例の活動性慢性炎症性脱髄性多発神経炎)を適合させると，非活動性 MS は全例健常人群に分類され，一方慢性炎症性脱髄性多発神経炎(chronic inflammatory demyelinating polyneuropathy：CIDP)は MS-A 群に分類された．

MMP-9 は IFN-β により低下，GA では上昇した．

van Boxel-Dezire ら[36]は IFN-β 治療を受けた 26 例の RRMS の PBMC におけるサイトカイン遺伝子発現レベルを半定量的 RT-PCR で経時的に解析した．治療前後 2 年間の再発回数・IVMP 回数・Extended Disability Status Scale(EDSS)スコアを集計し比較して 16 例のレスポンダーと 10 例のノンレスポンダーに分けると，レスポンダーは治療前に IL-12 p 35 発現レベルが低い傾向を呈した．Wandinger ら[37]は IFN-β 治療を受けた RRMS で治療後 1 年間再発がなく EDSS スコア悪化のみられない症例をレスポンダー，再発した症例をノンレスポンダーと定義した．20 例のレスポンダーと 19 例のノンレスポンダーを比較すると，レスポンダーでは TNF-related apoptosis-inducing ligand(TRAIL, TNFSF 10)が持続的高値を示すことを見出した．TRAIL は IRG の 1 つで，われわれ[18]は MS T 細胞における発現低下を報告している．TRAIL 遺伝子欠損マウスは胸腺細胞アポトーシスに異常をきたし，コラーゲン関節炎に高感受性になる[38]．Baranzini ら[39]は IFN β 治療を受けた 52 例の RRMS で PBMC における 70 遺伝子の発現レベルを経時的に定量的 RT-PCR で解析した．治療後 2 年間 1 度も再発がなく EDSS スコア悪化のない症例をレスポンダー，2 回以上再発した症例をノンレス

表 2. SVM 解析によるグループ分類

				Case No.	1	2	3	4	5	6	7	8	9	10	11
				Age/Sex	40 F	57 F	30 M	37 M	36 F	48 F	61 F	37 F	22 F	16 M	18 M
				Clinical Diagnosis	Active RRMS	Stable RRMS	Stable RRMS	Stable RRMS	Possible MS	Active RRMS	Stable RRMS	Possible MS	Optic Neuritis	CIDP	CIDP
				Clustering by 58 genes	A	Nc	Nc	Nc	A	Nc	Nc	Nc	Nc	A	A
SVM No.	Gene Set	Gene Selection Method	No. of Predictor Genes	Kernel Function	SVM Classification										
1	58	All genes	—	PDP(Order 1)	A	Nc	A	A	A	Nc	A	Nc	Nc	A	A
2	58	All genes	—	PDP(Order 2)	A	Nc	A	A	A	Nc	Nc	Nc	Nc	A	A
3	58	All genes	—	PDP(Order 3)	A	Nc	A	A	A	Nc	Nc	Nc	Nc	A	A
4	58	All genes	—	Radial basis(Gaussian)	A	Nc	A	A	A	Nc	Nc	Nc	Nc	A	A
5	286	All genes	—	PDP(Order 1)	A	Nc	A	A	A	Nc	Nc	Nc	Nc	A	A
6	286	All genes	—	PDP(Order 2)	A	Nc	A	A	A	Nc	Nc	Nc	Nc	A	A
7	286	All genes	—	PDP(Order 3)	A	Nc	A	A	A	Nc	Nc	Nc	Nc	A	A
8	286	All genes	—	Radial basis(Gaussian)	A	Nc	A	A	A	Nc	Nc	Nc	Nc	A	A
9	286	Fisher's Exact Test	50	PDP(Order 1)	A	Nc	A	Nc	A	Nc	Nc	Nc	Nc	A	A
10	286	Fisher's Exact Test	50	PDP(Order 2)	A	Nc	A	Nc	A	Nc	Nc	Nc	Nc	A	A
11	286	Fisher's Exact Test	50	PDP(Order 3)	A	Nc	A	Nc	A	Nc	Nc	Nc	Nc	A	A
12	286	Fisher's Exact Test	50	Radial basis(Gaussian)	A	Nc	A	Nc	A	Nc	Nc	Nc	Nc	A	A
13	286	Golub Method	50	PDP(Order 1)	A	Nc	A	A	A	Nc	Nc	Nc	Nc	A	A
14	286	Golub Method	50	PDP(Order 2)	A	Nc	A	A	A	Nc	Nc	Nc	Nc	A	A
15	286	Golub Method	50	PDP(Order 3)	A	Nc	A	A	A	Nc	Nc	Nc	Nc	A	A
16	286	Golub Method	50	Radial basis(Gaussian)	A	Nc	A	A	A	Nc	Nc	Nc	Nc	A	A
17	286	Fisher's Exact Test	30	PDP(Order 1)	A	Nc	A	Nc	A	Nc	Nc	Nc	Nc	A	A
18	286	Fisher's Exact Test	30	PDP(Order 2)	A	Nc	A	Nc	A	Nc	Nc	Nc	Nc	A	A
19	286	Fisher's Exact Test	30	PDP(Order 3)	A	Nc	A	Nc	A	Nc	Nc	Nc	Nc	A	A
20	286	Fisher's Exact Test	30	Radial basis(Gaussian)	A	Nc	A	Nc	A	Nc	Nc	Nc	Nc	A	A
21	286	Golub Method	30	PDP(Order 1)	A	Nc	A	Nc	A	Nc	Nc	Nc	Nc	A	Nc
22	286	Golub Method	30	PDP(Order 2)	A	Nc	A	Nc	A	Nc	Nc	Nc	Nc	A	Nc
23	286	Golub Method	30	PDP(Order 3)	A	Nc	A	Nc	A	Nc	Nc	Nc	Nc	A	Nc
24	286	Golub Method	30	Radial basis(Gaussian)	A	Nc	A	Nc	A	Nc	Nc	Nc	Nc	A	Nc
25	286	Fisher's Exact Test	10	PDP(Order 1)	A	Nc	A	Nc	A	Nc	Nc	Nc	Nc	A	A
26	286	Fisher's Exact Test	10	PDP(Order 2)	A	Nc	A	Nc	A	Nc	Nc	Nc	Nc	A	A
27	286	Fisher's Exact Test	10	PDP(Order 3)	A	Nc	A	Nc	A	Nc	Nc	Nc	Nc	Nc	Nc
28	286	Fisher's Exact Test	10	Radial basis(Gaussian)	A	Nc	A	Nc	A	Nc	Nc	Nc	Nc	Nc	Nc
29	286	Golub Method	10	PDP(Order 1)	A	Nc	A	Nc	A	Nc	Nc	A	Nc	A	Nc
30	286	Golub Method	10	PDP(Order 2)	A	Nc	A	Nc	A	Nc	Nc	A	Nc	A	Nc
31	286	Golub Method	10	PDP(Order 3)	A	Nc	A	Nc	A	Nc	Nc	Nc	Nc	A	Nc
32	286	Golub Method	10	Radial basis(Gaussian)	A	Nc	A	Nc	A	Nc	Nc	Nc	Nc	A	Nc
33	1259	All genes	—	PDP(Order 1)	A	A	A	A	A	A	Nc	Nc	Nc	A	A
34	1259	All genes	—	PDP(Order 2)	A	A	A	A	A	Nc	Nc	Nc	A	A	A
35	1259	All genes	—	PDP(Order 3)	A	A	A	A	A	Nc	Nc	A	A	A	A
36	1259	All genes	—	Radial basis(Gaussian)	A	A	A	A	A	Nc	Nc	Nc	A	A	A
37	1259	Fisher's Exact Test	50	PDP(Order 1)	A	Nc	A	A	A	Nc	Nc	Nc	Nc	A	A
38	1259	Fisher's Exact Test	50	PDP(Order 2)	A	Nc	A	A	A	Nc	Nc	Nc	Nc	A	A
39	1259	Fisher's Exact Test	50	PDP(Order 3)	A	Nc	A	A	A	Nc	Nc	Nc	Nc	A	A
40	1259	Fisher's Exact Test	50	Radial basis(Gaussian)	A	Nc	A	A	A	Nc	Nc	Nc	Nc	A	A
41	1259	Golub Method	50	PDP(Order 1)	A	Nc	A	Nc	A	Nc	Nc	Nc	Nc	A	A
42	1259	Golub Method	50	PDP(Order 2)	A	Nc	A	Nc	A	Nc	Nc	Nc	Nc	A	A
43	1259	Golub Method	50	PDP(Order 3)	A	Nc	A	A	A	Nc	Nc	Nc	Nc	A	A
44	1259	Golub Method	50	Radial basis(Gaussian)	A	Nc	A	A	A	Nc	Nc	Nc	Nc	A	A
45	1259	Fisher's Exact Test	30	PDP(Order 1)	A	Nc	A	A	A	Nc	Nc	Nc	Nc	A	A
46	1259	Fisher's Exact Test	30	PDP(Order 2)	A	Nc	A	A	A	Nc	Nc	Nc	Nc	A	A
47	1259	Fisher's Exact Test	30	PDP(Order 3)	A	Nc	A	A	A	Nc	Nc	Nc	Nc	A	A
48	1259	Fisher's Exact Test	30	Radial basis(Gaussian)	A	Nc	A	A	A	Nc	Nc	Nc	Nc	A	A
49	1259	Golub Method	30	PDP(Order 1)	A	Nc	A	Nc	A	Nc	Nc	Nc	Nc	A	A
50	1259	Golub Method	30	PDP(Order 2)	A	Nc	A	Nc	A	Nc	Nc	Nc	Nc	A	A
51	1259	Golub Method	30	PDP(Order 3)	A	Nc	A	Nc	A	Nc	Nc	Nc	Nc	A	A
52	1259	Golub Method	30	Radial basis(Gaussian)	A	Nc	A	Nc	A	Nc	Nc	Nc	Nc	A	A
53	1259	Fisher's Exact Test	10	PDP(Order 1)	A	Nc	A	Nc	A	Nc	Nc	Nc	Nc	A	A
54	1259	Fisher's Exact Test	10	PDP(Order 2)	A	Nc	A	Nc	A	Nc	Nc	Nc	Nc	A	A
55	1259	Fisher's Exact Test	10	PDP(Order 3)	A	Nc	A	Nc	A	Nc	Nc	Nc	Nc	A	A
56	1259	Fisher's Exact Test	10	Radial basis(Gaussian)	A	Nc	A	Nc	A	Nc	Nc	Nc	Nc	A	A
57	1259	Golub Method	10	PDP(Order 1)	Nc	Nc	Nc	Nc	Nc	Nc	Nc	Nc	Nc	A	Nc
58	1259	Golub Method	10	PDP(Order 2)	A	Nc	A	Nc	A	Nc	Nc	Nc	Nc	A	Nc
59	1259	Golub Method	10	PDP(Order 3)	A	Nc	A	Nc	A	Nc	Nc	Nc	Nc	A	Nc
60	1259	Golub Method	10	Radial basis(Gaussian)	A	Nc	A	Nc	A	Nc	Nc	Nc	Nc	A	A

未治療 MS(n=72)と健常人 Nc(n=22)の T 細胞の cDNA マイクロアレイ(1,259 遺伝子)解析で発現差異を認める 286 遺伝子を指標遺伝子(discriminator genes)とする階層的クラスター解析(hierarchical clustering analysis)で，MS 群は Nc 群と分離され A，B，C，D の 4 群に分類された．A 群は遺伝子発現プロフィールが最も Nc 群に類似し，群間検定で両者を識別する 58 遺伝子を抽出した．Gene Set：SVM 実行に使用された遺伝子セット，Gene Selection Method：predictor genes を選定した検定法，Kernel Function：グループ・クラス判別に使用された Kernel 関数の種類

ポンダーと定義し，両者は3遺伝子［caspase 2, caspase 10, FLICE inhibitory protein (FLIP)］の発現レベルの三次元マッピングで86%区別可能と報告した．

最近，われわれ[18]は72例のIFN-β未治療活動性MS(46例は初回採血後2年間IFN-β治療開始)と22名の健常人の末梢血CD 3+ T細胞を1,259遺伝子cDNAマイクロアレイ(Hitachi)で解析したデータに関して，両群間で発現差異を示す286遺伝子を指標遺伝子(discriminator genes)にして階層的クラスター解析を施行した［MS classification database (MSCD), Satoh *et al*, Manuscript in preparation］．286遺伝子は5クラス(クラス#1～#5)に分類され，MS群は健常人群から分離され，さらに4グループ(A, B, C, D)に分類された．A群は遺伝子発現プロフィールが最も健常人に類似し，B群は最も臨床的活動性が高く，ケモカイン遺伝子の多いクラス#5の発現レベルが高く，C群は大脳限局病変を呈する患者が多く，D群は最もEDSSスコアが高値であった．さらに群間検定で健常人とMS A群を識別する58遺伝子を抽出した．治療前後2年間の再発回数・IVMP日数・入院日数・EDSSスコア・MRI T2強調画像病巣数と患者満足度から治療評価スコアを算出すると，レスポンダーはA群とB群に集積していた．レスポンダーではノンレスポンダーに比較して，治療開始後6ヵ月のIRG (ISG 15, IFI 27, MCP-1, TNFRp 75)発現レベルが高く維持されていた．

このMSCDに新規11症例(2例の活動性MS, 4例の非活動性MS, 2例のpossible MS, 1例の視神経炎, 2例の活動性慢性炎症性脱髄性多発神経炎)を適合させると，286遺伝子，58遺伝子を指標遺伝子とする階層的クラスター解析により，非活動性MSは全例健常者群に分類された(**図1**)．一方慢性炎症性脱髄性多発神経炎(chronic inflammatory demyelinating polyneuropathy：CIDP)はMS A群に分類された．MSCDをtraining setとして施行したSVM解析でも同様のグループ分類が支持された(**表2**)．症例数は少ないがわれわれの結果は末梢神経抗原に対する自己免疫機序が関与するCIDPと中枢神経抗原に対する自己免疫機序が関与するMSではT細胞遺伝子発現レベルで類似性があり，CIDPはDNAマイクロアレイ解析だけではMSと鑑別できないことを示唆する．

おわりに

遺伝子アレイ解析は臨床所見や画像のみでは鑑別困難な疾患の補助診断のツール，腫瘍悪性度や予後の予測，薬物反応性や副作用の予測，治療効果の判定など幅広い臨床応用が期待されている．われわれはDNAマイクロアレイ解析でMSがT細胞遺伝子発現プロフィールにもとづき4群に分類され，各群は疾患活動性・病変分布・IFN-β治療反応性と密接な対応を認めることを報告した(MS classification database：MSCD)．今後MSCDを礎にしてテーラメイド医療樹立に向けて研究を進める予定である．

謝　辞：本稿で紹介した研究は，国立精神・神経センター神経研究所免疫研究部山村 隆部長，古池史子先生，中西恵美先生，尾上祐行先生，土居芳充先生，南里悠介先生，佐藤和気郎先生，荒浪利昌先生，および難治性疾患の画期的診断・治療法などに関する研究班の班員諸氏との共同研究でなされ，平成17年度厚生労働科学研究費補助金こころの健康科学(遺伝子アレイによる多発性硬化症再発予測法樹立に関する研究：H 17-こころ-020)および平成17年度創薬などヒューマンサイエンス総合研究事業(DNAマイクロアレイによる多発性硬化症の迅速診断法の樹立に関する研究：KH 21101)の補助を受けた．

文　献

1) Sospedra M *et al*：Immunology of multiple sclerosis. *Annu Rev Immunol* **23**：683-747, 2005
2) Waubant E *et al*：Clinical characteristics of

responders to interferon therapy for relapsing MS. *Neurology* **61**：184-189, 2003
3) Lucchinetti C *et al*：Heterogeneity of multiple sclerosis lesions：implications for the pathogenesis of demyelination. *Ann Neurol* **47**：707-717, 2000
4) Steinman L *et al*：Transcriptional analysis of targets in multiple sclerosis. *Nat Rev Immunol* **3**：483-492, 2003
5) Whitney AR *et al*：Individuality and variation in gene expression patterns in human blood. *Proc Natl Acad Sci USA* **100**：1896-1901, 2003
6) Whitney LW *et al*：Analysis of gene expression in multiple sclerosis lesions using cDNA microarrays. *Ann Neurol* **46**：425-428, 1999
7) Whitney LW *et al*：Microarray analysis of gene expression in multiple sclerosis and EAE identifies 5-lipoxygenase as a component of inflammatory lesions. *J Neuroimmunol* **121**：40-48, 2001
8) Chabas D *et al*：The influence of the proinflammatory cytokine osteopontin on autoimmune demyelinating disease. *Science* **294**：1731-1735, 2001
9) Lock C *et al*：Gene-microarray analysis of multiple sclerosis lesions yields new targets validated in autoimmune encephalomyelitis. *Nat Med* **8**：500-508, 2002
10) Mycko MP *et al*：cDNA microarray analysis in multiple sclerosis lesions：detection of genes associated with disease activity. *Brain* **126**：1048-1057, 2003
11) Graumann U *et al*：Molecular changes in normal appearing white matter in multiple sclerosis are characteristic of neuroprotective mechanisms against hypoxic insult. *Brain Pathol* **13**：554-573, 2003
12) Lindberg RL *et al*：Multiple sclerosis as a generalized CNS disease-comparative microarray analysis of normal appearing white matter and lesions in secondary progressive MS. *J Neuroimmunol* **152**：154-167, 2004
13) Tajouri L *et al*：Quantitative and qualitative changes in gene expression patterns characterize the activity of plaques in multiple sclerosis. *Mol Brain Res* **119**：170-183, 2003
14) Ramanathan M *et al*：*In vivo* gene expression revealed by cDNA arrays：the pattern in relapsing-remitting multiple sclerosis patients compared with normal subjects. *J Neuroimmunol* **116**：213-219, 2001
15) Airla N *et al*：Suppression of immune system genes by methylprednisolone in exacerbations of multiple sclerosis. Preliminary results. *J Neurol* **251**：1215-1219, 2004
16) Bomprezzi R *et al*：Gene expression profile in multiple sclerosis patients and healthy controls：identifying pathways relevant to disease. *Hum Mol Genet* **12**：2191-2199, 2003
17) Mayne M *et al*：CYFIP 2 is highly abundant in CD 4^+ cells from multiple sclerosiss patients and is involved in T cell adhesion. *Eur J Immunol* **34**：1217-1227, 2004
18) Satoh J *et al*：Microarray analysis identifies an aberrant expression of apoptosis and DNA damage-regulatory genes in multiple sclerosis. *Neurobiol Dis* **18**：537-550, 2005
19) Achiron A *et al*：Blood transcriptional signatures of multiple sclerosis：unique gene expression of disease activity. *Ann Neurol* **55**：410-417, 2004
20) Achiron A *et al*：Understanding autoimmune mechanisms in multiple sclerosis using gene expression microarrays：treatment effect and cytokine-related pathways. *Clin Dev Immunol* **11**：299-305, 2004
21) Mandel M *et al*：Autoimmunity gene expression portrait：specific signature that intersects or differentiates between multiple sclerosis and systemic lupus erythematosus. *Clin Exp Immunol* **138**：164-170, 2004
22) Maas K *et al*：Cutting edge：molecular portrait of human autoimmune disease. *J Immunol* **169**：5-9, 2002
23) Iglesias AH *et al*：Microarray detection of E 2 F pathway activation and other targets in multiple sclerosis peripheral blood mononuclear cells. *J Neuroimmunol* **150**：163-177, 2004
24) Satoh J *et al*：Differing effects of IFNβ vs IFNγ in MS. Gene expression in cultured astrocytes. *Neurology* **57**：681-685, 2001
25) Wandinger KP *et al*：Complex im-

munomodulatory effects of interferon-β in multiple sclerosis include the upregulation of T helper 1-associated marker genes. *Ann Neurol* **50**: 349-357, 2001
26) Koike F *et al*: Microarray analysis identifies interferon β-regulated genes in multiple sclerosis. *J Neuroimmunol* **139**: 109-118, 2003
27) Taniguchi T *et al*: The interferon-α/β system in antiviral responses: a multimodal machinery of gene regulation by the IRF family of transcription factors. *Curr Opin Immunol* **14**: 111-116, 2002
28) Maric M *et al*: Defective antigen processing on GILT-free mice. *Science* **294**: 1361-1365, 2001
29) Behar SM *et al*: Susceptibility of mice deficient in CD1D or TAP1 to infection with *Mycobacterium tuberculosis*. *J Exp Med* **189**: 1973-1980, 1999
30) Bárdos T *et al*: Anti-inflammatory and chondroprotective effect of TSG-6(tumor necrosis factor-α-stimulated gene-6)in murine models of experimental arthritis. *Am J Pathol* **159**: 1711-1721, 2001
31) Baechler EC *et al*: Interferon-inducible gene expression signature in peripheral blood cells of patients with severe lupus. *Proc Natl Acad Sci USA* **100**: 2610-2615, 2003
32) Weinstock-Guttman B *et al*: Genomic effects of IFN-β in multiple sclerosis patients. *J Immunol* **171**: 2694-2702, 2003
33) Liang Y *et al*: Differential and trajectory methods for time course gene expression data. *Bioinformatics* **21**: 3009-3016, 2005
34) Stürzebecher S *et al*: Expression profiling identifies responder and non-responder phenotypes to interferon-β in multiple sclerosis. *Brain* **126**: 1419-1429, 2003
35) Hong J *et al*: Gene expression profiling of relevant biomarkers for treatment evaluation in multiple sclerosis. *J Neuroimmunol* **152**: 126-139, 2004
36) van Boxel-Dezaire AH *et al*: Contrasting response to interferon β-1 b treatment in relapsing-remitting multiple sclerosis: does baseline interleukin-12 p 35 messenger RNA predict the efficacy of treatment? *Ann Neurol* **48**: 313-322, 2000
37) Wandinger KP *et al*: TNF-related apoptosis inducing ligand(TRAIL)as a potential response marker for interferon-beta treatment in multiple sclerosis. *Lancet* **361**: 2036-2043, 2003
38) Lamhamedi-Cherradi SE *et al*: Defective thymocyte apoptosis and accelerated autoimmune diseases in TRAIL$^{-/-}$mice. *Nat Immunol* **4**: 256-260, 2003
39) Baranzini SE *et al*: Transcription-based prediction of response to IFNβ using supervised computational methods. *PLoS Biol* **3**: e 2, 2005

神経内科，64(3)：319-320，2006

LETTERS TO THE EDITOR

DNAマイクロアレイによる多発性硬化症の診断とインターフェロンベータ治療反応性予測に関するアンケート調査

〔Questionnaires on the expediency of DNA microarray analysis for diagnosis of multiple sclerosis and prediction of therapeutic response to interferon-beta.〕

南里悠介　佐藤準一
佐藤和貴郎　山村　隆

〔Yusuke NANRI, M.D., Jun-ichi SATOH, M.D., Ph.D., Wakiro SATO, M.D. & Takashi YAMAMURA, M.D., Ph.D.: 国立精神・神経センター神経研究所免疫研究部(〒187-8502 東京都小平市小川東町4-1-1)；Department of Immunology, National Institute of Neuroscience, NCNP, Kodaira, Tokyo 187-8502, Japan〕

2006年1月17日

拝　啓

最近，多発性硬化症(multiple sclerosis：MS)前駆病態と考えられるclinically isolated syndrome(CIS)で，早期にインターフェロンベータ(interferon-beta：IFNB)治療を開始するとdefinite MSへの移行を抑制可能と報告されています[1]．しかし，本邦では視神経脊髄型MS(opticospinal MS：OSMS)が比較的多いので，早期診断はMcDonald診断基準では困難であり，有効な補助診断法の樹立が必要です．また，IFNBが無効な症例や副作用で使用できない症例も存在し，治療反応性予知法の確立が重要な課題です．現在ゲノムプロジェクト完了によりヒト全遺伝子塩基配列が解明され，遺伝子アレイ(DNAマイクロアレイまたはGene Chipと呼ばれる)を用いて個々の細胞における数万遺伝子(ヒト全遺伝子約30,000)の発現情報を包括的・系統的に解析可能になっております．このような網羅的発現解析により従来の研究方法では予期しなかった遺伝子のMS病態における役割が次々明らかにされ，薬物反応性の個人差が予測可能になりつつあります[2]．最近私どもは，末梢血T細胞マイクロアレイ解析によりMSにおけるアポトーシス制御遺伝子群の発現異常を報告しています[3]．

私どもは，神経内科専門医常勤1,709施設を対象に，DNAマイクロアレイによるMS診断法開発に対する期待感およびIFNB治療に関する現況を把握するためにアンケート調査を行い，319施設から回答を得ました．調査は以下の18項目(質問に対するyes/noとコメント記入)を含みます．[Q1]MSと腫瘍の鑑別が問題になった症例の経験がある．[Q2]その場合の診断法．[Q3]MSと脳血管障害の鑑別が問題になった症例の経験がある．[Q4]その場合の診断法．[Q5]MSか否か鑑別に苦慮する症例を診療している．[Q6]鑑別診断困難な理由．[Q7]T細胞マイクロアレイ解析によるMS補助診断法に興味がある．[Q8]外来診療MS患者数．[Q9]IFNB投与通算患者数．[Q10]治療結果に満足している患者数．[Q11]IFNB治療中に副作用などで中止となった経験がある．[Q12]その内容．[Q13]IFNBを積極的に治療に導入する．[Q14]消極的な理由．[Q15]IFNB有効性・副作用予測法開発を期待する．[Q16]患者からIFNB治療導入の相談を受け保留している例がある．[Q17]その理由．[Q18]T細胞マイクロアレイ解析によるIFNB治療効果・副作用予測法に興味がある．

その結果，171施設で腫瘍との鑑別が問題となり，70施設では生検が施行されていました．また，180施設で脳血管障害との鑑別が問題となり，4施設で生検が施行されていました．102施設で鑑別診断困難症例を経験しており，9施設がSjøgren症候群との鑑別に言及していました．IFNB